AD-A120 112 FOREST PRODUCTS LAB MADISON WI F/G 11/12
EFFECT OF KNOTS ON STRESS WAVES IN LUMBER.(U)
SEP 82 C C GERHARDS
UNCLASSIFIED FSRP-FPL-384 NL

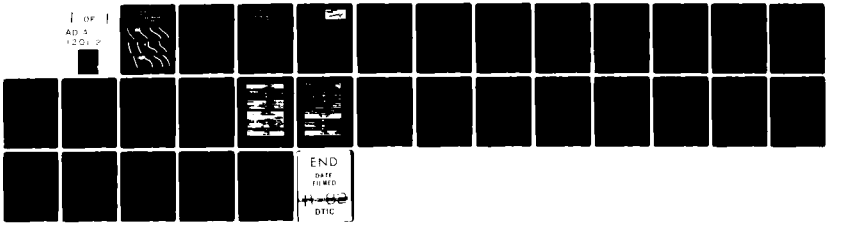

United States
Department of
Agriculture

Forest Service

Forest
Products
Laboratory

Research
Paper
FPL 384

Effect of Knots on Stress Waves in Lumber

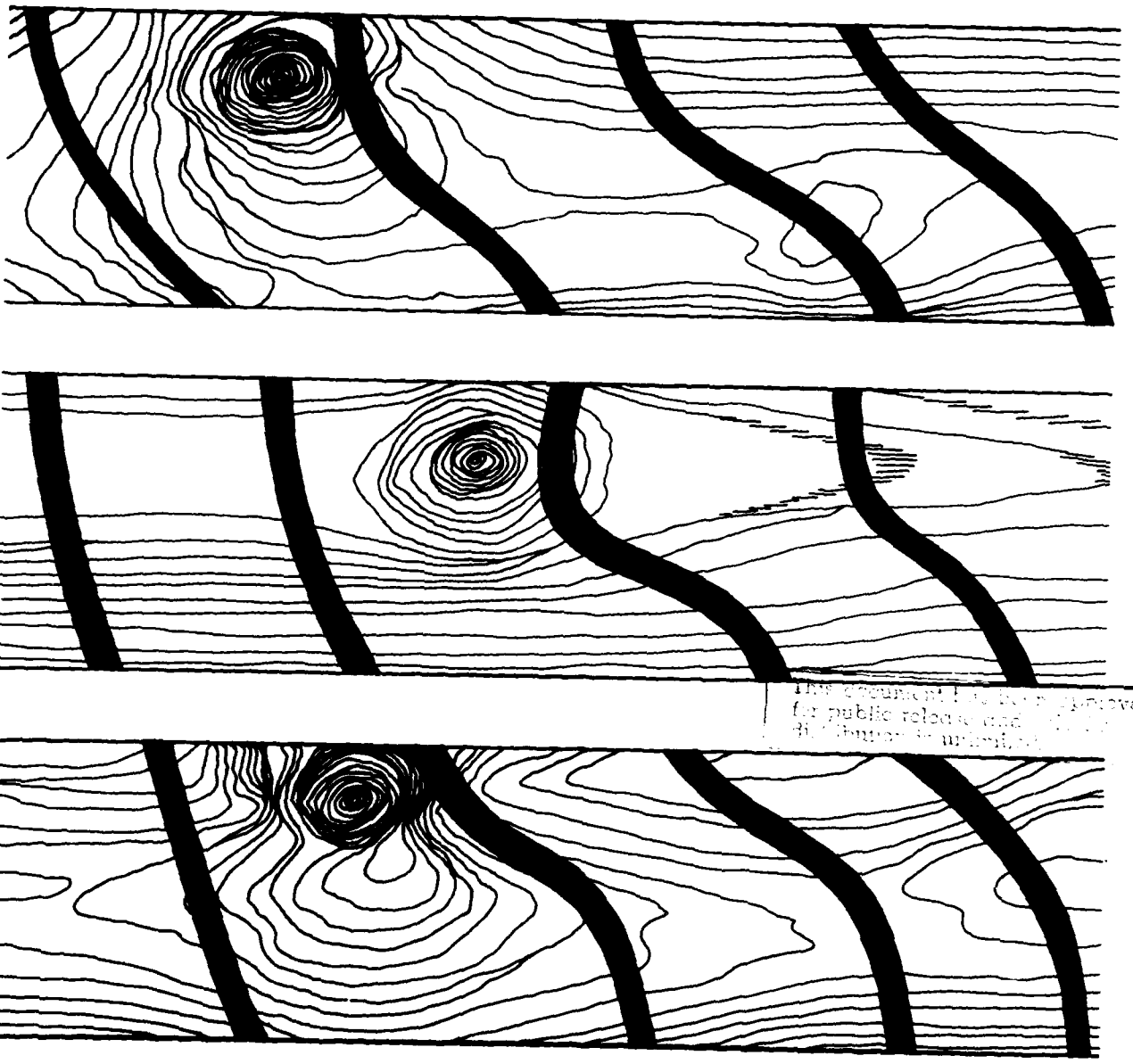

Abstract

An impact stress wave was induced in the end of 2 by 6 lumber containing knots. Rather than a normal, perpendicular-to-the-axis profile in transiting by a knot, the stress wave tended to lead in zones of clear wood in the direction of the slope of grain or slope of the annual rings and to lag behind the knot. Of three methods evaluated to time the stress wave, the "average" timing method was more consistent than other methods in flagging the 6-inch length containing a knot from adjacent clear wood 6-inch lengths. Stress wave modulus of elasticity (ESW) calculated from the data tended to be lowest with the average timing method. All ESW's were higher than ESB (static bending modulus of elasticity); however, the two types of moduli tended to approach each other as knots were removed by ripping away successive 3/4-inch strips down to a specimen width of 1-3/4-inches. The results of this study should provide guidance in establishing stress wave methods for machine grading of lumber.

United States
Department of
Agriculture

Forest Service

Forest
Products
Laboratory[1]

Research
Paper
FPL 384

September 1982

Effect of Knots on Stress Waves in Lumber

By
C. C. GERHARDS, Engineer

Introduction

Although stress waves have been proposed as a means for rapid machine stress rating of lumber, the concept has seen only limited commercial application. A better understanding of how stress waves propagate and interact with characteristics inherent in lumber should enhance the commercial use of stress wave-techniques for lumber grading. Previous reports on stress waves were concerned with lumber elasticity or with the effects of moisture content, annual rings, or slope of grain in lumber (*1,2,3,4*).[2] This report is concerned with propagation of stress waves in lumber containing knots and how the propagation characteristics may be used to determine a modulus of elasticity based on stress waves. A static bending modulus of elasticity is included for comparison. The study is based on an evaluation of eleven 8-foot long flatsawn 2 by 6's that were subsequently ripped in five stages down to a width of about 1-3/4 inches, with reevaluation after each stage.

Descriptions

Sample

Of the 11 flatsawn 2 by 6's, 9 were southern pine and 2 were Douglas-fir. Except for one specimen that contained two knots at one cross section and another specimen that contained only a small portion of an edge knot, each of the specimens contained a single prominent knot located more or less in the middle-third length. A brief description of knot and slope of grain characteristics of each specimen is given in appendix A.

[1] Maintained at Madison, Wis., in cooperation with the University of Wisconsin.

[2] Italicized numbers in parentheses refer to literature cited at the end of this report.

Stress Wave Method

The stress-wave equipment used in this study was developed at Washington State University (fig. 1). It induces a compressive impact stress wave in the end of a specimen when a solenoid activated hammer strikes a steel wedge clamped to one end of a specimen. Two accelerometers are fastened to the specimen some distance apart to sense passage of the stress wave. The accelerometer nearer to the hammer end (the impact end) starts a microsecond counter and the accelerometer farther from the hammer end stops the microsecond counter as the stress wave advances past each accelerometer. Thus, the microsecond counter times the stress wave as it travels the distance between the two accelerometers.

Experimental Procedures

The specimens were conditioned to and maintained at equilibrium in a controlled 75° F, 50 percent relative humidity atmosphere throughout the study. Seven longitudinal grid lines 3/4 inch apart were drawn over a 2-1/2-foot test length on both pithside and barkside of each specimen (fig. 2). Cross-section lines 6 inches apart intersected the 3/4-inch grid lines making 42 grid points on each wide face. The 6-inch cross-section lines were numbered consecutively from 1, farthest to the left of the knot, to 6, farthest to the right of the knot; the knot was centered between 6-inch cross-section lines 3 and 4. The 3/4-inch grid lines were also numbered consecutively, from 1 through 7; 3/4-inch grid line 1 was near the edge farthest from the knot (fig. 2).

Weight and dimensions of each of the 11 specimens were measured. Transit time of the impact stress wave was then measured with both the left and then the right end acting as the hammer end. For the transit time measurement the start accelerometer was mounted on the centerline of the barkside wide face 6 inches from the end being impacted; the stop accelerometer was

mounted at random on each of the 84 grid points. An impact stress wave was induced for each grid point transit-time measurement. By trial and error, the transit time was also determined where the stress wave first arrived at each 6-inch cross-section line; this measurement will be referred to as "fastest point" timing. Because slope of grain affects stress wave transit (2), the stress wave was timed on both wide faces. This procedure allowed study of the three-dimensional interaction of the stress wave with the knot and cross grain due to fiber angle and annual ring slope.

Following the transit-time measurements, the central 70-inch length of each specimen was subjected to a uniform bending moment of about 325 inch-pounds per inch of width (equivalent to about 900 lb/in.^{2} bending stress) for determining the flatwise static load-deflection characteristics of the 2-1/2-foot test length (fig. 3). In this test the deflections of 6-inch cross-section lines (CX) 2, 3, 4, and 5 were measured relative to the adjacent 6-inch cross-section lines to allow calculation of moduli of elasticity for four overlapping 1-foot lengths.

Measurements of weight, dimensions, load-deflection characteristics, and transit times to all remaining grid points were repeated after each of five successive 3/4-inch wide strips were ripped from the edge opposite 3/4-inch grid line 1. Thus, final measurements were made on essentially knot free wood having about a 1-3/4 inch width that contained grid lines 1 and 2. Finally, coupons were cut from each specimen to determine moisture content by the ovendry method.

Calculations

Moisture content, gross density (including moisture content), knot area ratios, stress-wave contours, stress-wave times for a 6- inch transit distance, and modulus of elasticity were calculated from the data. Knot area ratio (KAR) is the ratio of the area of the knot projected on a cross section to the cross sectional area of the piece. The static bending modulus of elasticity (ESB) was determined from

$$ESB = \frac{ML^2}{8I\delta} \qquad (1)$$

where M was the applied constant bending moment causing the deflection δ relative to the span length L equal to 12 inches and I was the flatwise moment of inertia for a specimen. From geometric arguments, it can be shown that a static bending modulus of elasticity for a 2-foot span under uniform moment can be estimated with very small error from

$$\text{2-foot ESB} = \frac{4}{\frac{1}{ESB_1} + \frac{2}{ESB_2} + \frac{1}{ESB_3}} \qquad (2)$$

where ESB_1 and ESB_3, are moduli for the first and second 1-foot lengths of the 2-foot span and ESB_2 is the modulus for the 1-foot span overlapping the inner 6

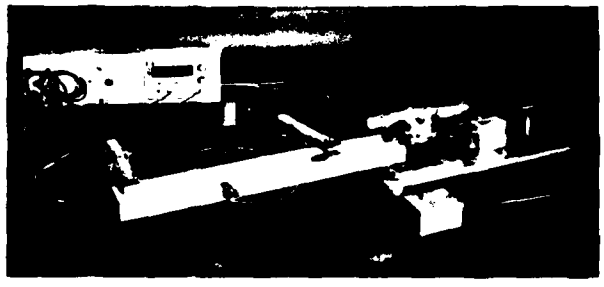

Figure 1.—Stress-wave equipment used to measure transit time (shown with a 2 by 4). (M 141881)

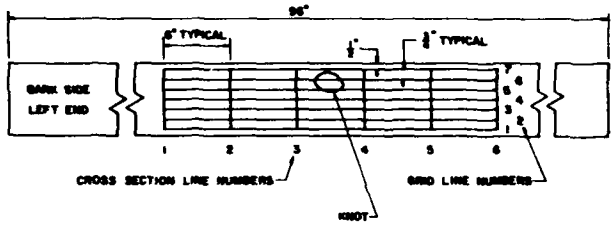

Figure 2.—Schematic showing the 42 grid points (formed by the intersections of 7 grid lines with 6 cross section lines) on barkside of an 8-foot 2 by 6. The same grid points were also located on the pithside. M 148 969

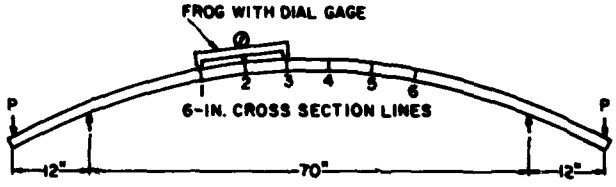

Figure 3.—Flatwise static bending test. The Frog shown spanning 6-inch cross-section lines 1, 2, and 3 measured deflection of line 2 relative to lines 1 and 3. Deflection was due to bending moment of loads P acting 12 inches outside support points. M 148 204

inches of each 1-foot length of the 2-foot span. An ESB was calculated by equation (2) for the left and right 2-foot portions of the 2-1/2-foot test length. Dynamic modulus of elasticity (ESW) based on the stress-wave data was calculated from

$$ESW = \rho C^2$$

where ρ is mass density and C the speed of the stress wave determined from the distance and transit-time measurements. Calculations of stress-wave contours and 6-inch transit times will be included in later discussions of the properties.

Results and Discussion

Moisture Content, Density, and Knot Area Ratio (KAR)

Moisture content averaged about 10 percent but varied between specimens from about 9-1/2 to 12 percent (table 1). Density calculated from specimen weight and volume measurements varied both between and within specimens (table 1). Between specimens, density ranged between 31 and 42 pounds per cubic foot; within specimens, density ranged between 97 and 105 percent of the density for the full 2-by-6 width, depending on specimen and ripped width. The greatest variation in density with ripped width occurred in specimens 6172, DF2, 6095, and 4050. KAR also varied with ripped width (table 1): 1) increasing as width was ripped down to 4 inches and decreasing as width was reduced further in the specimens where the prominent knot in the 2 by 6 was near midwidth (6047, DF1, 6172, 4086, and 4050); 2) decreasing as width was reduced where the prominent knot in the 2 by 6 was on the edge (5153, 4021, and 5154); or 3) decreasing then increasing followed by decreasing as width was reduced where two prominent knots occurred in the 2 by 6 (6095).

Static Bending Modulus of Elasticity (ESB)

Several trends are apparent in the ESB values for 1-foot increments or spans (table 2). First, in the wider specimens (5.5 inches down to a ripped specimen width of at least 3-1/4 inches) the ESB values were lower in the two 1-foot spans containing the prominent knot (second and third foot increments) than in the two 1-foot spans away from the prominent knot (first and fourth foot increments). The trend in specimen 4021 is an exception, probably due to the small portion of edge knot present in the full specimen width. Second, ESB values tended to change systematically as a

Table 1.—Some physical aspects of test specimens as 2 by 6's and after successive 3/4-inch strips were ripped off

Specimen number	Moisture content	Approximate width	Density	Knot area ratio	Specimen number	Moisture content	Approximate width	Density	Knot area ratio
	Pct	In.	Lb/ft³			Pct	In.	Lb/ft³	
6047	9.9	5.50	34.8	0.27	4021	9.5	5.50	32.5	0.07
		4.75	34.9	.31			4.75	32.6	.00
		4.00	34.7	.37			4.00	32.9	.00
		3.25	35.0	.23			3.25	32.9	.00
		2.50	35.3	.00			2.50	33.0	.00
		1.75	35.4	.00			1.75	33.4	.00
DF1	11.7	5.50	39.7	.24	6095	9.5	5.50	39.6	.20
		4.75	39.8	.28			4.75	39.7	.12
		4.00	39.3	.32			4.00	39.9	.13
		3.25	39.7	.22			3.25	40.6	.16
		2.50	39.7	.04			2.50	41.4	.19
		1.75	40.1	.00			1.75	41.5	.09
4107	10.2	5.50	33.7	.31	4086	9.6	5.50	33.3	.32
		4.75	33.8	.37			4.75	33.2	.37
		4.00	33.6	.23			4.00	33.1	.38
		3.25	33.4	.03			3.25	33.2	.23
		2.50	33.2	.00			2.50	33.7	.02
		1.75	33.4	.00			1.75	33.0	.00
5153	9.9	5.50	31.2	.35	5154	9.9	5.50	39.4	.31
		4.75	31.3	.23			4.75	39.3	.22
		4.00	31.2	.10			4.00	39.1	.08
		3.25	30.9	.00			3.25	38.7	.00
		2.50	31.3	.00			2.50	38.8	.00
		1.75	31.6	.00			1.75	38.7	.00
6172	11.0	5.50	32.5	0.26	4050	10.2	5.50	32.3	0.29
		4.75	32.5	.30			4.75	32.2	.33
		4.00	32.7	.36			4.00	32.3	.39
		3.25	32.9	.22			3.25	33.0	.29
		2.50	33.5	.02			2.50	34.0	.09
		1.75	34.2	.00			1.75	32.2	.00
DF2	10.3	5.50	36.0	.20					
		4.75	36.2	.24					
		4.00	36.4	.26					
		3.25	36.4	.30					
		2.50	36.4	.06					
		1.75	34.9	.00					

Table 2.—ESB values for 1-foot portions of the 2-1/2-foot test section

Specimen number	Approximate width	ESB for 1-foot increment number[1]				Specimen number	Approximate width	ESB for 1-foot increment number[1]			
		1	2	3	4			1	2	3	4
	In.	---------10^6 Lb/in.^{2}---------					In.	---------10^6 Lb/in.^{2}---------			
6047	5.50	2.11	1.94	1.94	2.05	4021	5.50	1.67	1.54	1.48	1.78
	4.75	2.12	1.77	1.89	2.10		4.75	1.68	1.54	1.55	1.77
	4.00	2.12	1.71	1.81	2.16		4.00	1.71	1.67	1.54	1.66
	3.25	2.04	2.06	2.01	2.08		3.25	1.64	1.68	1.69	1.73
	2.50	2.25	2.27	2.25	2.16		2.50	1.53	1.61	1.72	1.64
	1.75	2.35	2.40	2.31	2.23		1.75	1.57	1.61	1.71	1.63
DF1	5.50	2.00	1.66	1.49	1.71	6095	5.50	2.40	2.06	1.81	2.10
	4.75	1.98	1.55	1.44	1.62		4.75	2.41	2.21	1.94	2.13
	4.00	1.93	1.40	1.33	1.61		4.00	2.44	2.21	2.04	2.31
	3.25	2.01	1.53	1.45	1.61		3.25	2.46	2.25	2.02	2.46
	2.50	1.86	1.66	1.54	1.59		2.50	2.60	2.29	2.09	2.63
	1.75	1.74	1.63	1.64	1.74		1.75	2.61	2.48	2.29	2.82
4107	5.50	2.16	1.70	1.67	2.02	4086	5.50	1.55	1.44	1.28	1.85
	4.75	2.12	1.60	1.68	1.96		4.75	1.75	1.32	1.22	1.78
	4.00	2.04	1.71	1.79	1.93		4.00	1.82	1.24	1.17	1.76
	3.25	2.02	1.82	1.90	2.06		3.25	1.87	1.42	1.18	1.77
	2.50	2.09	1.89	1.98	2.09		2.50	2.01	1.59	1.26	1.84
	1.75	1.99	1.92	2.06	2.10		1.75	2.14	1.83	1.39	1.88
5153	5.50	1.51	1.08	1.06	1.88	5154	5.50	2.37	1.62	1.50	2.01
	4.75	1.55	1.09	1.11	1.84		4.75	2.44	1.69	1.54	2.02
	4.00	1.55	1.18	1.19	1.88		4.00	2.50	1.87	1.66	2.12
	3.25	1.40	1.35	1.27	1.78		3.25	2.55	1.99	1.82	2.13
	2.50	1.46	1.36	1.38	1.83		2.50	2.58	2.14	2.00	2.32
	1.75	1.42	1.47	1.46	1.80		1.75	2.60	2.22	2.11	2.48
6172	5.50	1.87	1.46	1.53	1.67	4050	5.50	1.57	1.39	1.43	1.93
	4.75	1.93	1.41	1.47	1.73		4.75	1.55	1.28	1.36	1.91
	4.00	1.91	1.42	1.54	1.79		4.00	1.55	1.23	1.32	1.94
	3.25	1.93	1.49	1.67	1.88		3.25	1.65	1.27	1.39	1.92
	2.50	2.15	1.61	1.86	1.96		2.50	1.75	1.48	1.63	2.09
	1.75	2.18	1.82	1.97	2.04		1.75	1.81	1.60	1.72	1.97
DF2	5.50	2.43	2.28	2.32	2.64						
	4.75	2.38	2.19	2.28	2.55						
	4.00	2.32	2.02	2.18	2.50						
	3.25	2.41	1.96	1.96	2.38						
	2.50	2.38	2.21	2.21	2.46						
	1.75	2.39	2.35	2.27	2.37						

[1] One-foot increment number 1 lies between 3-inch grid lines 1 and 3, 2 between grid lines 2 and 4, 3 between grid lines 3 and 5, and 4 between grid lines 4 and 6.

specimen's width was reduced by ripping. An example is specimen 5153 in which the clear wood ESB values tended to decrease slightly as width was reduced, whereas, the ESB values for foot increments 2 and 3 (containing the knot) increased as width was reduced. Third, in a few specimens such as 4086, ESB values were substantially different in the two 1-foot clear wood sections adjacent to the knot and in clear wood beside the knot, that is, when the knot has been removed by the ripping sequence. Fourth, when ESB values for foot increments 2 and 3 are compared to the KAR values in table 1, it is apparent that ESB tended to increase as KAR decreased in a specimen due to ripping to different widths. This fourth trend is also apparent in ESB values based on a 2-foot span length and calculated from equation (2). The ESB values for 2-foot spans are tabulated in a later table along with stress-wave E values.

To quantify the trend noted between ESB and KAR for a specimen, the ESB values for the left 1-foot span containing the knot (foot increment number 2) and the ESB values for the left 2-foot span (foot increments 1, 2, and 3— table 2) were each fit to the KAR values by least squares in the simple regression ESB= A+ B (KAR) for each specimen across all widths. Regression results by specimen and length of span are given in table 3. Because each regression is based on only six data points, that is, one point per specimen width, any coefficient of determination (r^2) below about 0.81 is not significantly different from zero at the 5 percent level of significance. Consequently, the regression results for specimens DFI, DF2, 402l, and 6095 are not considered significant by themselves. The lack of significance for specimen 402l is not surprising due to the shallow portion of edge knot in the full specimen width. The result for specimen 6095 may be due to a poor estimate of

Table 3.—Regressions of ESB on KAR for the left 1-foot and 2-foot spans containing the knot[1]

Specimen number	Left 1-foot span				Left 2-foot span			
	A	B	r^2[2]	S_{yx}[3]	A	B	r^2[2]	S_{yx}[3]
6047	2.35	-1.66	0.94	0.077	2.31	-1.30	0.97	0.042
DF1	1.67	- .52	.47	.082	1.68	- .37	.42	.063
4107	1.89	- .72	.93	035	1.95	- .57	.94	.027
5153	1.37	- .98	.81	.079	1.38	- .73	.82	.056
6172	1.72	- .96	.83	.073	1.86	-1.03	.89	.061
DF2	2.36	-1.03	.67	.097	2.35	- .70	.56	.083
4021	1.62	-1.17	.31	.056	1.63	- .94	.42	.035
6095	2.57	-2.17	.46	.113	2.53	-1.95	.39	.116
4066	1.72	-1.13	.84	.093	1.67	- .85	.85	.068
5154	2.09	-1.67	.86	.100	2.15	-1.49	.84	.096
4050	1.59	- .91	.92	.045	1.67	- .92	.98	.023

[1] ESB in 10^6 lb/in.^{2} and KAR in fractions.

[2] Values below 0.81 not significant at 5 percent level.

[3] Standard deviation about the regression.

the KAR portion for the overgrown knot. Overall, however, the regression results for the majority of the specimens imply a significant increasing trend in ESB with a decrease in KAR, as would be expected.

Stress-Wave Contours

If contours of constant stress-wave transit times were mapped, they would reveal how the stress wave advances along the length of a specimen. To physically locate such contours, however, it would have been necessary to make many trial and error measurements with the apparatus available for measuring transit time. It is possible to estimate contours from the grid point transit-time data from

$$D_j = \bar{t}\,(d/t_j) \qquad (4)$$

where $\bar{t}$ is the average of transit times to all grid points at a cross section d distant from the start or reference accelerometer, t_j is the transit time to one of the grid points, and D_j is the estimated distance to the stress-wave contour having transit time $\bar{t}$.

Figure 4 shows an example of estimated contours about the 6-inch cross-section lines for one specimen (5153), full width, with the left end of the specimen as the hammer end, that is with the stress wave advancing from left to right. Simple stress wave theory presumes that the stress wave should advance with a normal front, that is, the contour should be a line perpendicular to the direction of stress wave transit. The contour about CX1 (fig. 4) suggests some deviation from a normal front in that the stress wave tended to lead along the lower edge and to lead on the barkside.

The influence of the knot is strongly reflected as a distortion in the stress-wave contour immediately "downstream" from the knot (CX4), compared to the contour immediately "upstream (CX3) (fig. 4). That response was somewhat typical for most of the specimens. In some, however, the knot influence was masked somewhat by slope of grain effect (*2*), as contours tended to lead in the direction of slope of the fibers or annual rings. The annual ring slope effect was evident in the leading or lagging characteristics of the contours on either the barkside or the pithside of a specimen, the fiber slope effect by a sloping contour. In a few of the specimens, stress-wave contours "upstream" from the knot suggested the possibility of a nonnormal induced stress wave at the impact end. Due to the geometry of the gripping apparatus through which the stress wave was induced, it is possible that in a specimen with cupped ends, the stress wave could initially lead along the centerline of the specimen or at two points near the edges, depending on cup orientation (*2*).

Stress-Wave Transit Times For 6-Inch Transit

Although stress-wave contours are of fundamental concern, a best way of measuring transit time must be gleaned from the data if a stress-wave modulus of elasticity is to be determined. Because of the different possible ways of commercially applying stress waves, three different timing measures are considered: (1) fastest point time, because it represents the earliest arrival of the stress wave at a 6-inch CX line whether on barkside or pithside—based on the trial and error data; (2) average time, because it tends to give equal weight to both the leading and the lagging portions of the stress wave—based on a simple average of the transit time measurements to the grid points on a 6-inch CX line on both barkside and pithside; (3) centerline time on a wide face, because it represents the simplest form of timing—based on the time to each 6-inch CX line at

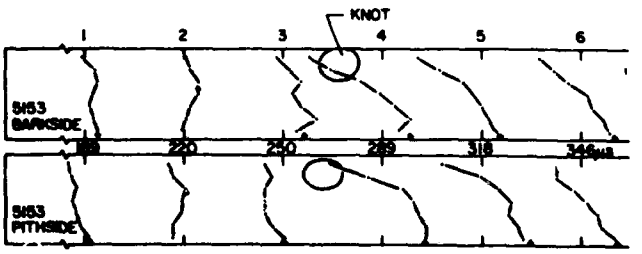

Figure 4.—Estimated stress wave contours (— · — · —) on barkside and pithside about 6 cross sections in a 2 by 6 containing a knot. Stress wave advanced from left to right.
M 148 968

midwidth. Results for centerline time are considered separately for barkside and pithside. The differences in times between consecutive 6-inch CX lines for any one timing basis represent the 6-inch transit times and are given in appendix C for all possible variables.

Fastest Point 6-inch Transit Time—Fastest point timing must be considered inconsistent in detecting the knot section from other 6-inch sections in the study lumber. Based on averages across widths (table 4), the fastest point transit times for only three of the specimens (DF1, 5153, and 5154 in table 4) were generally longer ($\geq$2 μs) for the knot section than for the average clear wood 6-inch section regardless of hammer end; fastest point transit times for three of the specimens (6172, 4021, and 4050) were generally no longer (<2 μs) for the knot section than for the average clear wood 6-inch section regardless of hammer end. In three of the other specimens (6047, 4107, and DF2) the fastest point transit times were shorter for the knot section than for the average clear wood 6-inch section for one or the other hammer end.

One other interesting aspect that reflects inconsistency in fastest point timing is the difference in times for the 6-inch knot section due to hammer end. Based on the averages for the fastest point times over all specimen widths that contained knot portions (table 4), the difference due to hammer end amounted to between 3 to 5 μs in four of the specimens (6047, 4107, 4086, and 5154); in only one specimen was there no difference (6095). The above observations suggest, as the contours illustrate, that grain slope and clear wood affect fastest point timing much more than knots do.

Average Time for 6-inch Transit—Average timing for 6 inches of transit was fairly consistent in reflecting the presence of the knot. Based on averages across widths (table 5) in seven specimens (DF1, 4107, 5153, 6095, 4086, 5154, and 4050), the average times for 6 inches of transit were generally longer ($\geq$2 μs) for the 6-inch section containing the knot than for the average clear wood 6-inch section regardless of hammer end. In only one specimen (6172) was the average time for the knot section shorter than for the average clear wood 6-inch section for one or the other hammer end.

Hammer end had less effect on transit time for the 6-inch section containing the knot when based on average timing than when based on fastest point timing. None of the specimens had greater than 2 μs difference due to hammer end for average timing, based on the data in table 5.

Tables 4 and 5 reveal that stress wave transit times are generally shorter for fastest point timing than for average timing, as expected.

Table 4.—Averages of 6-inch transit times in microseconds (fastest point procedure) demonstrating effects of knot and hammer end[1]

Specimen number	Number of widths[2]	Hammer end left		Hammer end right	
		All clear wood[3]	Knot[4]	All clear wood[3]	Knot[4]
6047	4	27.9	30.2	28.1	26.5
DF1	5	32.2	38.0	32.8	38.6
4107	4	26.9	32.0	26.6	27.2
5153	3	29.7	32.7	29.6	37.3
6172	5	26.4	27.0	29.4	27.6
DF2	5	25.6	29.5	27.8	27.4
4021	1	31.6	32.0	30.8	30.0
6095	6	27.4	30.3	26.4	30.3
4086	5	29.9	30.8	30.0	34.2
5154	3	27.2	29.7	29.8	34.3
4050	5	29.0	30.6	29.0	29.4

[1] Based on data contained in appendix C.

[2] For all those widths of specimen containing any portion of the knot.

[3] Averages based on transit times between cross sections 1 and 2, 2 and 3, 4 and 5, and 5 and 6.

[4] Averages based on transit times between cross sections 3 and 4.

Table 5.—Averages of 6-inch transit times in microseconds (average procedure) demonstrating effects of knot and hammer end[1]

Specimen number	Number of widths[2]	Hammer end left		Hammer end right	
		All clear wood[3]	Knot[4]	All clear wood[3]	Knot[4]
6047	4	27.9	30.2	27.8	29.5
DF1	5	33.1	36.2	32.8	36.0
4107	4	28.2	32.8	28.1	31.2
5153	3	29.8	36.0	29.4	34.3
6172	5	28.7	29.2	29.4	29.0
DF2	5	26.8	30.2	27.2	28.0
4021	1	31.0	32.0	31.5	32.0
6095	6	27.5	31.0	28.4	31.3
4086	5	29.7	34.8	30.8	34.2
5154	3	27.4	33.7	28.8	34.3
4050	5	29.4	31.4	29.1	33.0

[1] Based on data contained in appendix C.

[2] For all those widths of specimen containing any portion of the knot.

[3] Averages based on transit times between cross sections 1 and 2, 2 and 3, 4 and 5, and 5 and 6.

[4] Averages based on transit times between cross sections 3 and 4.

Exceptions may be noted, however, where there is no difference in times or average timing yields the shorter value. Identical values will result when stress wave contours maintain the same shape with transit distance. Average timing will yield the shorter value when slope of the stress wave contour decreases with transit distance.

Centerline 6-inch Transit Time—If the barkside only is considered, centerline timing for 6 inches of transit was about as good as the average time basis for reflecting the presence of the knot. Based on averages across widths (table 6), eight of the specimens (DF1, 4107, 5153, 4021, 6095, 4086, 5154, and 4050), had centerline times generally longer (≥ 2 μs) on the barkside for the 6-inch section containing the knot than for the average clear wood 6-inch section, regardless of hammer end. In two of the specimens (6172 and DF2), however, the barkside centerline times were shorter for the knot section than for the average clear wood 6-inch section for one or the other hammer end.

If the pithside only is considered, centerline timing for 6 inches of transit must be considered inconsistent in detecting the knot section from other 6-inch sections. Based on averages across widths (table 6), only three specimens (DF1, DF2, and 6095) had centerline pithside times generally longer (≥ 2 μs) in the 6-inch knot section than in the average clear wood 6-inch section, regardless of hammer end. However, there were eight specimens (6047, 4107, 5153, 6172, 4021, 4086, 5154, and 4050) where the pithside centerline times were shorter for the knot section than for the average clear wood 6-inch section for one or the other hammer end.

If centerline timing is based on the shortest time considering both the barkside and pithside together, it is not very consistent in detecting the knot section. While the data are not given here, only six of the knot sections (DF1, 4107, 5153, 6095, 4086, and 5154) would have been detected with one of the hammer ends and none with the other hammer end.

Based on averages for the times over all specimen widths that contain knot portions (table 6) the differences in times for the 6- inch knot section, due to hammer end, amounted to between 4 to 5 μs in three specimens (6172, DF2, and 5154) for barkside and between 4 to 6 μs in four specimens (DF1, 6172, 4021, and 5154) for pithside timing, reflecting a trend similar to that for fastest point timing.

Transit Time Over the Full 2-1/2-foot Test Section

Based on the differences in times to the first and the sixth cross section lines, stress-wave times for the 2-1/2-foot test length (table 7) depended to some extent on hammer end and to a lesser extent on timing basis

Table 6.—Averages of 6-inch transit times in microseconds (centerline basis) demonstrating effects of knot and hammer end[1]

Specimen number	Number of widths[2]	Barkside				Pithside			
		Hammer end left		Hammer end right		Hammer end left		Hammer end right	
		All clear wood[3]	Knot[4]	All clear wood[3]	Knot[4]	All clear wood[3]	Knot[4]	All clear wood[3]	Knot[4]
6047	4	27.8	29.7	27.9	29.7	28.1	29.3	27.5	27.0
DF1	5	32.7	36.7	33.3	36.3	32.9	39.7	32.7	35.0
4107	4	28.2	32.3	28.0	33.3	29.2	29.3	28.5	28.0
5153	3	29.1	41.0	27.4	40.0	30.9	26.0	31.9	26.5
6172	5	29.0	26.7	29.1	31.3	28.3	30.7	29.9	25.3
DF2	5	26.6	29.7	27.3	25.7	26.8	31.0	27.2	31.3
4021	1	30.5	33.0	30.5	35.0	30.2	31.0	31.8	26.0
6095	6	27.3	32.7	26.5	32.3	27.2	31.7	28.1	31.3
4086	5	29.0	37.7	29.8	38.7	30.9	30.7	31.7	30.0
5154	3	26.9	34.0	27.4	38.5	28.6	30.5	30.0	24.5
4050	5	28.9	34.3	29.3	34.3	30.8	29.0	28.6	31.7

[1] Based on data contained in appendix C.

[2] For all those widths of specimen containing any portion of the knot.

[3] Averages based on transit times between cross sections 1 and 2, 2 and 3, 4 and 5, and 5 and 6.

[4] Averages based on transit times between cross sections 3 and 4.

Table 7.—Transit times for the 2-1/2-foot test length versus specimen width—differences between transit times to the first and sixth cross-section lines

Specimen number	Approximate width	Fastest point timing basis		Average timing basis		Centerline timing basis			
						Hammer end left		Hammer end right	
		Hammer end left	Hammer end right	Hammer end left	Hammer end right	Barkside	Pithside	Barkside	Pithside
	In.	μs							
6047	5.50	143	136	142	141	142	143	145	139
	4.75	144	140	144	141				
	4.00	141	139	142	141	141	141	142	138
	3.25	139	140	140	140				
	2.50	137	139	140	137	139	141	137	134
	1.75	138	136	138	137				
DF1	5.50	157	169	164	165	166	170	168	162
	4.75	165	168	167	169				
	4.00	174	173	171	170	168	173	170	172
	3.25	173	170	171	166				
	2.50	164	170	170	167	168	171	171	163
	1.75	170	167	170	166				
4107	5.50	152	140	148	144	149	150	146	144
	4.75	147	142	146	145				
	4.00	146	145	144	143	145	144	147	141
	3.25	145	142	144	143				
	2.50	142	141	144	142	142	144	143	141
	1.75	144	143	145	143				
5153	5.50	151	155	157	154	158	153	151	157
	4.75	152	154	155	152				
	4.00	151	151	154	150	157	148	148	151
	3.25	151	149	154	149				
	2.50	152	149	153	152	155	151	150	148
	1.75	153	151	153	151				
6172	5.50	143	145	146	147	145	143	148	148
	4.75	141	143	144	146				
	4.00	142	146	144	147	142	143	147	143
	3.25	141	146	143	146				
	2.50	142	146	143	146	141	146	148	144
	1.75	145	144	144	145				
DF2	5.50	130	140	135	136	135	133	137	140
	4.75	132	139	137	137				
	4.00	131	137	137	136	135	141	134	141
	3.25	135	139	138	137				
	2.50	136	139	140	137	138	141	134	139
	1.75	140	136	141	136				
4021	5.50	155	154	156	154	155	152	157	153
	4.75	150	155	152	152				
	4.00	151	154	153	152	155	153	156	149
	3.25	152	149	151	151				
	2.50	156	155	157	153	156	157	156	148
	1.75	155	153	159	153				
6095	5.50	139	142	143	145	144	144	147	145
	4.75	139	144	142	146				
	4.00	138	144	141	145	141	141	146	147
	3.25	140	144	140	146				
	2.50	140	147	139	144	141	137	146	139
	1.75	144	143	142	143				
4086	5.50	149	154	153	158	155	153	155	157
	4.75	151	154	154	158				
	4.00	152	154	156	159	153	158	163	161
	3.25	150	153	153	156				
	2.50	150	155	152	155	153	152	156	152
	1.75	153	155	153	155				

(Page 1)

Table 7.—Transit times for the 2-1/2-foot test length versus specimen width—differences between transit times to the first and sixth cross-section lines—continued

Specimen number	Approximate width	Fastest point timing basis		Average timing basis		Centerline timing basis			
						Hammer end left		Hammer end right	
		Hammer end left	Hammer end right	Hammer end left	Hammer end right	Barkside	Pithside	Barkside	Pithside
	In.	μs							
5154	5.50	138	154	145	149	143	146	148	145
	4.75	138	153	143	149				
	4.00	139	153	142	150	140	144	148	145
	3.25	139	152	140	149				
	2.50	140	152	140	150	139	143	151	147
	1.75	138	151	139	151				
4050	5.50	147	147	150	150	150	150	154	149
	4.75	145	145	149	150				
	4.00	147	145	149	150	151	147	151	152
	3.25	146	146	148	149				
	2.50	148	145	148	148	149	148	148	147
	1.75	147	146	147	147				

(Page 2)

and specimen width. The most striking hammer end effect occurred for specimen 5154; end differences averaged 14 μs for fastest point time and 8 μs for both average time and barkside centerline time. It may be noted that the shorter transit times for 5154 and some others favored the end closer to the knot. The shorter transit times for six of the specimens (6047, DF1, 5153, DF2, 4021, and 4050), however, were generally not consistent with the shorter distance of the knot section from the hammer end.

Of the three timing procedures, none is consistent in favoring a shorter or longer time for the 2-1/2-foot transit distance. Considering the data of table 7 overall, fastest point timing gave slightly shorter transit times than average timing for either end to the hammer in five of the specimens (6047, 6172, 6095, 4086, and 4050) but only by about 1 to 3 μs, an insignificant amount. Centerline timing generally had slightly shorter transit times than average timing when the lower of the barkside and pithside centerline values are considered; however, average timing values tended to be shorter than the higher of the barkside and pithside centerline timing values.

The variation in the transit time data of table 7 with specimen width is not particularly consistent with how knot-area ratio (KAR) changed with specimen width (table 1). This relationship will be discussed further in the following section dealing with correlations.

Correlation of 6-inch or 2-1/2-foot Transit Time Values with KAR

Based on simple correlations between KAR and stress-wave times either for the 6-inch length containing the knot (tables 4 and 5) or for the 2-1/2-foot length (table 7), the coefficients of determination (r^2) shown in table 8 generally suggest poor correlations between transit time and KAR. All r^2 values marked as significant in table 8 have a positive correlation between transit time and KAR, that is, as knot-area ratio increased, transit time increased. Many of the r^2 values that lack significance, however, are for negative correlations, even the relatively high value of 0.72 for specimen 6095.

As a very general observation of table 8 data, average timing seems to be a better choice for detecting knot size than fastest point timing. This conclusion is supported by both the number of significant r^2 values and the number of positive correlations. For average timing the 6- inch times seem to offer a moderate advantage over the 2-1/2-foot times in correlating with KAR; there does not appear to be any transit-distance preference for fastest point timing. Centerline timing was not correlated with KAR because only three data sets for any one specimen-end-side combination were obtained.

ESW Compared to ESB—1-foot Span Basis

ESW calculated by equation (3) and based on 1-foot transit times can be compared directly with ESB given in table 2 for the same 1-foot spans. The four 1-foot spans and the six specimen widths for each specimen provide 24 sets of ESW-ESB data for comparison for both fastest point timing and average timing for each end to the hammer; only 12 sets are available for centerline timing because centerline times apply to only three specimen widths (0, 2, and 4 strips removed). As it would be difficult to visually compare ESW with ESB due to the multitude of data, only the r^2 values will be presented; these values give a general picture of how the two types of E's correlate on the 1-foot span basis.

While most of the r^2 values (table 9) are significant in a statistical sense, ESW would generally seem to be a poor predictor of ESB within a specimen, at least on a

Table 8—Coefficients of determination between transit time for the 6-inch or 2-1/2-foot length containing the knot and knot-area ratio[1]

Specimen number	Distance of transit time measurement							
	6 inches				2-1/2 feet			
	Fastest point timing		Average timing		Fastest point timing		Average timing	
	Hammer end left	Hammer end right	Hammer end left	Hammer end right	Hammer end left	Hammer end right	Hammer end left	Hammer end right
6047	0.14	0.07-[2]	0.91*[3]	0.75	0.65	0.64	0.12	0.96*
DF1	.30	.20-	.95*	.08-	.00	.06-	.27	.25
4107	.39	.02	.95*	.64	.60	.44	.00-	.73
5153	.91*	.18	.97*	.94*	.14-	.90*	.90*	.55
6172	.06	.01	.70	.35	.33-	.12	.00	.58
DF2	.08-	.09-	.15-	.08	.56-	.54-	.17	.05
4021	.64	.28	1.00*	.45	.13	.04	.02	.49
6095	.72-	.05	.05	.62	.24-	.06-	.05	.06
4086	.08	.05	.54	.86*	.05-	.49	.45-	.90*
5154	.03	.23-	.89*	.70	.36-	.93*	.77	.36-
4050	.01-	.31	.85*	.43	.26-	.58	.00-	.92*

[1] Each value based on 6 data sets.

[2] Values followed by a minus sign indicate a negative correlation.

[3] Values with an asterisk are significant at 5 percent level or better.

1-foot span basis. The best value of r^2 at 0.86 (ESW based on centerline timing, barkside, hammer end left for specimen 5153) would be considered good by itself; however, r^2's are low or insignificant for many of the specimens. Some even suggest a negative correlation. Considering all specimens, the average timing basis seems to have produced the best ESW-ESB correlations. The general observation can also be made that barkside centerline timing usually yielded better correlations than pithside centerline timing.

ESW Compared to ESB—2-foot Span Basis

As ESB values could be calculated from 1-foot span ESB's and equation (2) for a 2-foot span, ESW values were calculated by equation (3) for the same 2-foot length, based on the three different transit time measures, but only for left end to hammer (appendix D). The values of ESW by fastest point and average timing for the 2-foot spans are shown in figure 5 as a function of specimen width along with ESB for comparison.

The general similarity in the figure 5 ESB curves between the left and right 2-foot sections of the 2-1/2-foot test section for a specimen is due basically to the relatively smooth trend of ESB with length as shown in table 2 and the 1-1/2-foot length that is common to each left and right 2-foot span length. The left and right 2-foot span ESW curves are not so similar as those for ESB.

Figure 5 curves have some other trends worth noting: 1) ESB was consistently less than ESW; 2) ESW based on fastest point times tended to be greater than ESW based on average times, but not consistently so; 3) trends in the ESW values based on average times were generally more closely related to trends in the ESB values than were trends in the ESW values based on fastest point times, but neither type of ESW appeared to be consistently well related to ESB, reinforcing the results determined in the 1-foot span evaluation considered earlier; 4) ESW generally tended to approach ESB as specimen width approached 1.75 inches; this relationship, in conjunction with KAR data in table 1, suggests that the two measures of elasticity were more nearly alike in clear wood than in wood-containing knots.

In support of the trend noted in item 3) above, correlations of ESW and ESB within specimens for 2-foot spans were generally not statistically significant (5 pct level), so are not shown here. The within-specimen r^2 values tended to be higher for ESW based on average time than for ESW based on fastest point time.

With the data for all specimens and widths combined, correlations between ESW and ESB, regardless of timing base for ESW, were significant (table 10). Correlations of ESB on ESW based on average timing were

Table 9.—Coefficient of determination (r^2) between ESW and ESB, both based on equal 1-foot specimen lengths

Specimen number	For ESW based on: Fastest point timing[1]		Average timing[1]		Centerline timing[2]			
					Hammer end left		Hammer end right	
	Hammer end left	Hammer end right	Hammer end left	Hammer end right	Barkside	Pithside	Barkside	Pithside
6047	0.16	0.02	0.68	0.45	0.29	0.01	0.19	0.21
DF1	.72	.57	.67	.35	.47	.50	.51	.15
4107	.32	.07-[3]	.52	.62	.54	.04-	.62	.20
5153	.00	.03	.83	.42	.86	.38-	.80	.29-
6172	.06	.02-	.15	.01	.01-	.00	.11	.41-
DF2	.19	.03	.54	.16	.41	.38	.05-	.18
4021	.20	.05-	.19	.26	.22	.02	.41	.11-
6095	.21	.29	.65	.73	.69	.56	.59	.29
4086	.01	.40	.56	.59	.59	.03	.34	.00
5154	.20	.31	.51	.37	.76	.12	.50	.24-
4050	.15	.01-	.44	.76	.47	.10	.47	.33

[1] Values of $r^2 \geq 0.17$ significant at 5 percent level.

[2] Values of $r^2 \geq 0.33$ significant at 5 percent level.

[3] Values of r^2 with a following negative sign indicate a negative correlation.

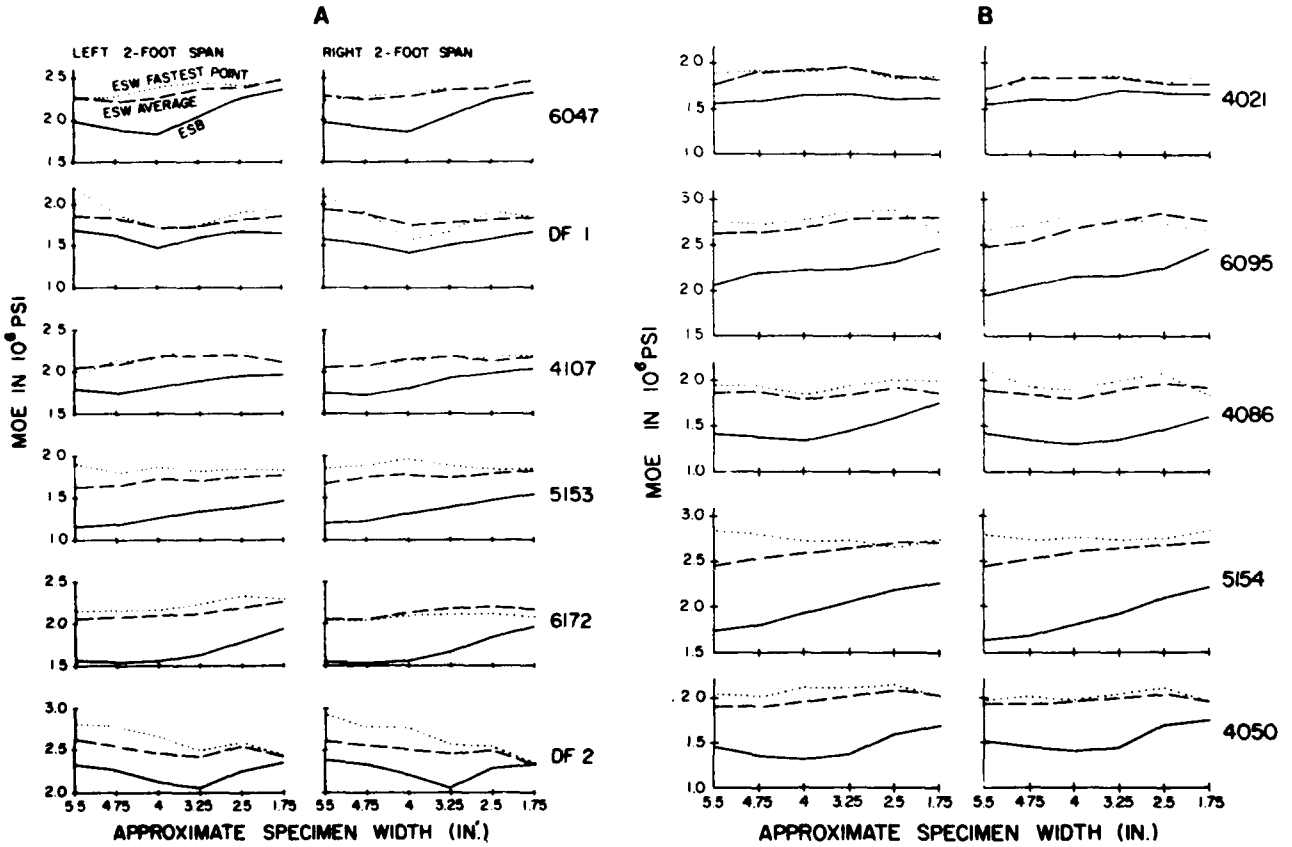

Figure 5.—ESB and ESW based on left end to the hammer and fastest point and average times for the left and right 2-foot portions of the 2-1/2-foot test section containing the knot. A.—Specimens 6047, DF1, 4107, 5153, 6172, and DF2. B.—4021, 6095, 4086, 5154, and 4050.
M 148 970, M 148 971

Table 10.—Overall regressions of ESB (Y) on ESW (X) based on Y = A + BX and the data of appendix D[1]

Variable for ESW	r^2	A	B	Average ESB	Average ESW	Coefficient of variation ESB	Coefficient of variation ESW
						Pct	Pct
BASED ON ALL WIDTHS							
Fastest point time, N = 66							
Left 2-foot span	0.66	0.04	0.77	1.77	2.24	19.0	15.7
Right 2-foot span	.59	.28	.67	1.76	2.21	18.3	16.7
Average time, N = 66							
Left 2-foot span	.79	-.11	.87	1.77	2.15	19.0	15.9
Right 2-foot span	.72	.00	.82	1.76	2.15	18.3	15.5
Centerline time, N = 33							
Barkside							
Left 2-foot span	.80	.02	.81	1.75	2.15	19.0	17.1
Right 2-foot span	.71	.02	.81	1.74	2.14	18.4	15.7
Pithside							
Left 2-foot span	.63	.05	.79	1.75	2.15	19.0	15.5
Right 2-foot span	.64	.14	.74	1.74	2.15	18.4	16.1
BASED ON 2-1/2-INCH WIDTH ONLY							
Centerline time, N = 11							
Barkside							
Left 2-foot span	.91	-.02	.84	1.87	2.23	17.9	16.9
Right 2-foot span	.84	.07	.82	1.86	2.18	17.1	16.2
Pithside							
Left 2-foot span	.78	.06	.83	1.87	2.20	17.9	16.3
Right 2-foot span	.68	.31	.70	1.86	2.22	17.1	17.0
BASED ON FULL WIDTH ONLY							
Fastest point, N = 11							
Left 2-foot span[2]	.53	.28	.63	1.70	2.25	19.5	17.0
Right 2-foot span[2]	.49	.52	.52	1.68	2.21	18.9	19.2
Average time, N = 11							
Left 2-foot span	.76	-.04	.83	1.70	2.10	19.5	16.6
Right 2-foot span	.69	-.04	.82	1.68	2.10	18.9	15.4
Centerline time, N = 11							
Barkside							
Left 2-foot span	.72	.18	.73	1.70	2.08	19.5	18.5
Right 2-foot span	.61	.09	.76	1.68	2.10	18.9	15.6
Pithside							
Left 2-foot span[2]	.43	.29	.67	1.70	2.11	19.5	15.5
Right 2-foot span	.60	.21	.70	1.68	2.10	18.9	16.7
BASED ON 1-3/4-INCH WIDTH ONLY							
Fastest point time, N = 11							
Left 2-foot span	.88	-.33	1.03	1.95	2.23	18.0	14.5
Right 2-foot span	.81	.14	.83	1.95	2.18	17.0	16.5
Average time, N = 11							
Left 2-foot span	.90	-.03	.90	1.95	2.20	18.0	16.8
Right 2-foot span	.86	.10	.85	1.95	2.18	17.0	16.6

[1] Based on ESB and ESW in 10^6 lb/in.^{2}

[2] r^2 and regression not significant at 5 percent level.

very similar for both the left and right 2-foot portions of the 2-1/2-foot test span, suggesting a relatively stable relation between the two variables. The results for centerline timing on the barkside were very similar to the average timing results. For the combined data the averages (table 10) show considerable discrepancy between ESW and ESB, with ESW averaging from 21 to 27 percent higher than ESB, depending on the timing method for ESW.

Correlations between ESW and ESB for the full-width data for the 11 specimens were not quite as good as those for all specimens and widths combined (table 10). In fact the two correlations for the fastest point timing basis and one correlation for the pithside centerline timing basis were not significant. The averages of ESW and ESB for the full-width data (table 10) show slightly more discrepancy than for all widths, with ESW averaging from 22 to 32 percent higher than ESB, depending on timing method for ESW.

Correlations between ESW and ESB for the narrowest width data for the 11 specimens essentially composed of clear wood were better than for either all widths combined or full width only (table 10); the best correlations occurred for average timing and barkside centerline timing. The averages of ESW and ESB for the narrowest width were closer together than for either all widths combined or full width only, ESW averaged from 12 to 19 percent higher than ESB. The higher correlations and closer averages for the narrow-width data support the trend noted above that stress-wave and static bending moduli were more nearly alike in clear wood than in wood containing a knot.

Conclusions

Several conclusions are warranted from the data of this study. Some of these generally dealing with static bending modulus of elasticity (ESB) and relative knot size (KAR) may not be new but they do support known trends. Among the most important conclusions are:

1. An impact stress wave induced in the end of lumber with knots does not maintain a normal perpendicular-to-the-axis profile in its transit by a knot and the cross grain associated with the knot. Contours of constant stress-wave transit time tend to lead in zones of clear wood in the direction of the slope of grain and slope of annual rings and lag behind the knot.

2. The sensitivity in detecting the presence of knots varies with timing procedures. Of three timing procedures evaluated, average timing appears more consistent in detecting short segments containing knots from adjacent clear wood segments than either fastest point or centerline timing.

3. Modulus of elasticity based on stress waves (ESW) tends to be higher than modulus of elasticity based on static bending (ESB), particularly in segments of lumber containing a knot.

4. The correlation between ESB and ESW depends greatly on specimen quality and stress wave timing procedure. ESB was best correlated with ESW based on average timing or barkside centerline timing and least correlated with ESW based on fastest point timing. In fact, ESB was only significantly correlated with ESW based on average timing or barkside centerline timing when specimens were full width with all the lumber characteristics. However, when the lumber was ripped to the narrowest width (clear wood only), ESB was significantly correlated with ESW regardless of timing procedures.

5. From impact tests on each end of a specimen, the direction of the impact stress wave affects transit timing somewhat. The differences in transit time for a given length of specimen due to impact end tended to be higher for fastest point timing than for average or centerline timing.

6. Stress wave timing is not very sensitive to relative knot size as correlations between knot-area ratio and transit time were generally poor to insignificant within a specimen.

7. Static bending E responded to the presence of knots or related grain distortion. ESB was lower for 1-foot spans containing a knot than for adjacent clear wood 1-foot spans. As espected, ESB increased systematically as knot-area ratio was reduced through ripping off 3/4-inch strips from the lumber.

As a general observation, some caution is suggested in applying stress wave techniques for machine stress rating lumber. Suitable devices could be developed for either average or fastest point timing. Otherwise, centerline timing could be used with accelerometers such as were used in this study, but grading might be less efficient than for average timing.

Some additional factors need to be evaluated: (1) depending on the size and soundness of a knot, stress-wave detection may be affected somewhat if the accelerometer fixed in a machine comes to rest on a knot; (2) to determine the effectiveness of grading that uses stress waves, ESW should be examined against lumber strength directly rather than by inference through ESB-strength relations. This approach is recommended due to the lack of perfect or near perfect correlation between ESW and ESB in typical lumber.

References

1. Galligan, W. L.; Courteau, R. W. Measurement of the elasticity of lumber with longitudinal stress waves and the piezoelectric effect of wood. Proc. 2nd Symp. on the Nondestructive Testing of Wood. Wash. State Univ. p. 223-244; 1965.

2. Gerhards, C. C. Effect of cross grain on stress waves in lumber. USDA For. Serv. Res. Pap. FPL 368, For. Prod. Lab., Madison, Wis.; 1980.

3. Gerhards, C. C. Effect of earlywood and latewood on stress-wave measurements parallel to the grain. Wood Sci. 11(2):69-72; 1978.

4. Gerhards, C. C. Stress wave speed and MOE of sweetgum ranging from 150 to 15 percent MC For. Prod. J. 25(4):51-57; 1975.

Appendix A: Specimen Descriptions

In the following brief descriptions of each specimen, left and right ends as pictured in figure 6, were maintained throughout the study. Slope of grain (fiber angle and annual ring slope) are described as positive or negative (fig. 7). A positive fiber angle, determined from resin canals or surface checks, implies that the grain, as seen on the barkside wide face when viewed relative to the barkside wide face, is directed from near the lower left corner of a specimen out near the upper right corner. A negative fiber angle implies the opposite direction. A positive annual ring slope implies that the annual ring, as seen on an edge, is directed from the pithside toward the left end out to the barkside toward the right end. A negative annual ring slope implies the opposite direction.

Specimen 6047.—The prominent knot, 1.45 inches in diameter, was located 58 inches from the left end and slightly off midwidth. The knot was intergrown on the pithside only. An overgrown 1/2-inch knot was located about 6 inches to the right of the prominent knot. Except for grain associated with the knots, there was almost no slope to the grain in 6047.

Specimen DF 1.—One of the two Douglas-fir specimens. The prominent knot, 1.30 inches in diameter, was located 44 inches from the left end and slightly off midwidth. The knot was only partly intergrown on the pithside. Slope of grain was variable. The fiber angle had a positive slope and was more severe on the barkside than on the pithside, ranging between 1 in 8 and 1 in 13-1/2 on the barkside and 1 in 10-1/2 and 1 in 24 on the pithside. A 1-foot length near the left end of the specimen had a negative annual ring slope ranging up to 1 in 12. A crook-in-tree caused annual ring deviation, centered about 15 inches toward the right end from the knot, had a maximum positive slope of about 1 in 4-1/2 and a negative slope somewhat less severe. A pithside surface check was also associated with the crook-in-tree ring deviation. To the right of the local crook, annual rings had a negative slope of about 1 in 13.

Specimen 4107.—The prominent knot, about 1.70 inches in diameter and completely intergrown, was located about 66-1/2 inches from the left end and was about 1 inch off midwidth. Fiber angle was essentially nil on the barkside and generally shallow and positive on the pithside with a maximum slope of 1 in 15-1/2 located near the left end. Annual ring slope was almost nil, except for a short section located about 2-1/2 feet toward the left end from the knot that had a positive slope of about 1 in 12-1/2 maximum.

Specimen 5153.—The prominent knot, about 1.90 inches in diameter and intergrown on the pithside only, was located on the edge of the specimen 62-1/2 inches from the left end. The fiber angle had a negative slope but was generally shallow, except for the slope on the barkside ranged between 1 in 8 and 1 in 14 over the mid 2-foot length and between 1 in 8-1/2 and 1 in 11 over the right end 2 feet of the specimen. Annual ring slope was essentially nil except for a short 1 in 4 negative sloping section immediately to the right of the knot.

Specimen 6172.—The prominent knot, 1.40 inches in diameter and completely intergrown, was located slightly off midwidth 34 inches from the left end. A 1/2-inch diameter knot was located about 12 inches toward the right end from the prominent knot. The fiber angle had a positive slope and was generally shallow, except for the slope on the pithside over the left 3-foot length that ranged between 1 in 8 and 1 in 12-1/2 with the barkside at about 1 in 15. Annual ring slope was essentially nil.

Specimen DF 2.—In this second Douglas-fir specimen the prominent knot, about 1.10 inches in diameter, encased and partly overgrown, was located about midlength and midwidth. Slopes of fiber angle and annual rings were almost nil except for the left 1-foot length that had fiber angle sloping about 1 in 13-1/2 and a short section just to the left of the knot that had fiber angle sloping about 1 in 9, both with positive slopes.

Specimen 4021.—This specimen contained only a small portion of a large knot that was located about 59-1/2 inches from the left end and at one edge of the piece. The specimen also contained a 1/2-inch knot along the opposite edge and 23 inches toward the left end from the prominent knot. Fiber angle and annual ring slopes were essentially nil to the left of the prominent knot. To the right of the knot, the fiber angle had a positive slope ranging between 1 in 11 and 1 in 20 on both barkside and pithside. There was also local annual ring curvature, about 15 inches toward the right end from the knot, probably caused by growth around or over a knot, with a maximum slope of 1 in 2 (negative).

Specimen 6095.—This specimen contained 2 prominent knots at the same cross section about 39 inches from the left end. Each knot was equivalent to about 1-inch diameter on the pithside. Both were intergrown on the pithside and one was overgrown on the barkside. A much smaller knot was located about 7 inches further to the right. Another small knot was located about 23 inches from the left end and a third smaller knot about 12 inches from the right end. Fiber angle and annual ring slopes were essentially nil, except for a short section near the right end that had a 1 in 13 positive fiber angle slope.

Specimen 4066.—The prominent knot, 1.72 inches in diameter, was located very slightly off midwidth about

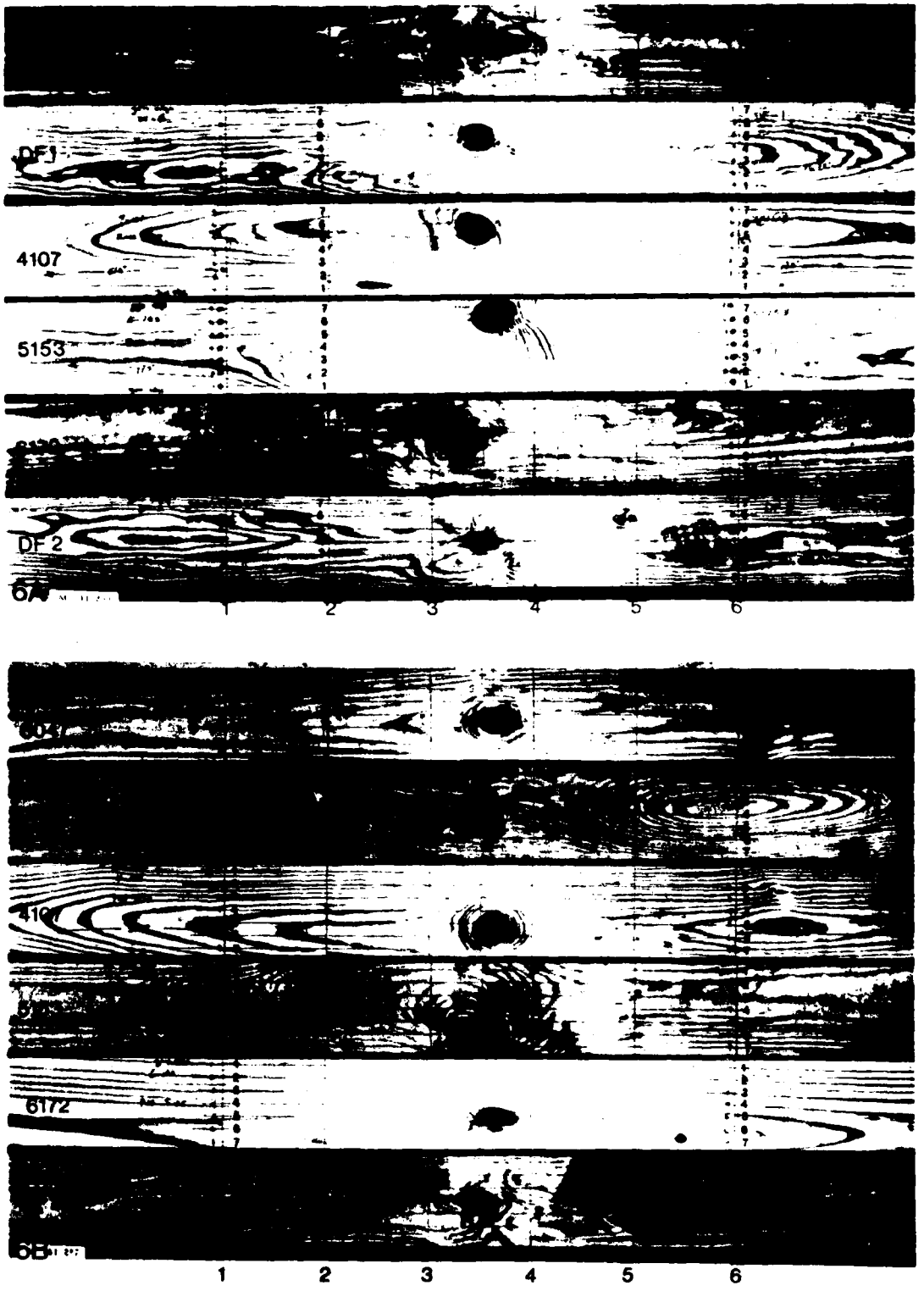

Figure 6.—Barkside and pithside views of the eleven 8-foot long 2 × 6's. Inscribed on each specimen are seven 3/4-inch grid lines (type set numbers) and six 6-inch cross-section lines over the 2-1/2-foot test section. A. barkside and B. pithside of 6047, DF1, 4107, 5153, 6172, and DF2.
M 141 254, M 141 253

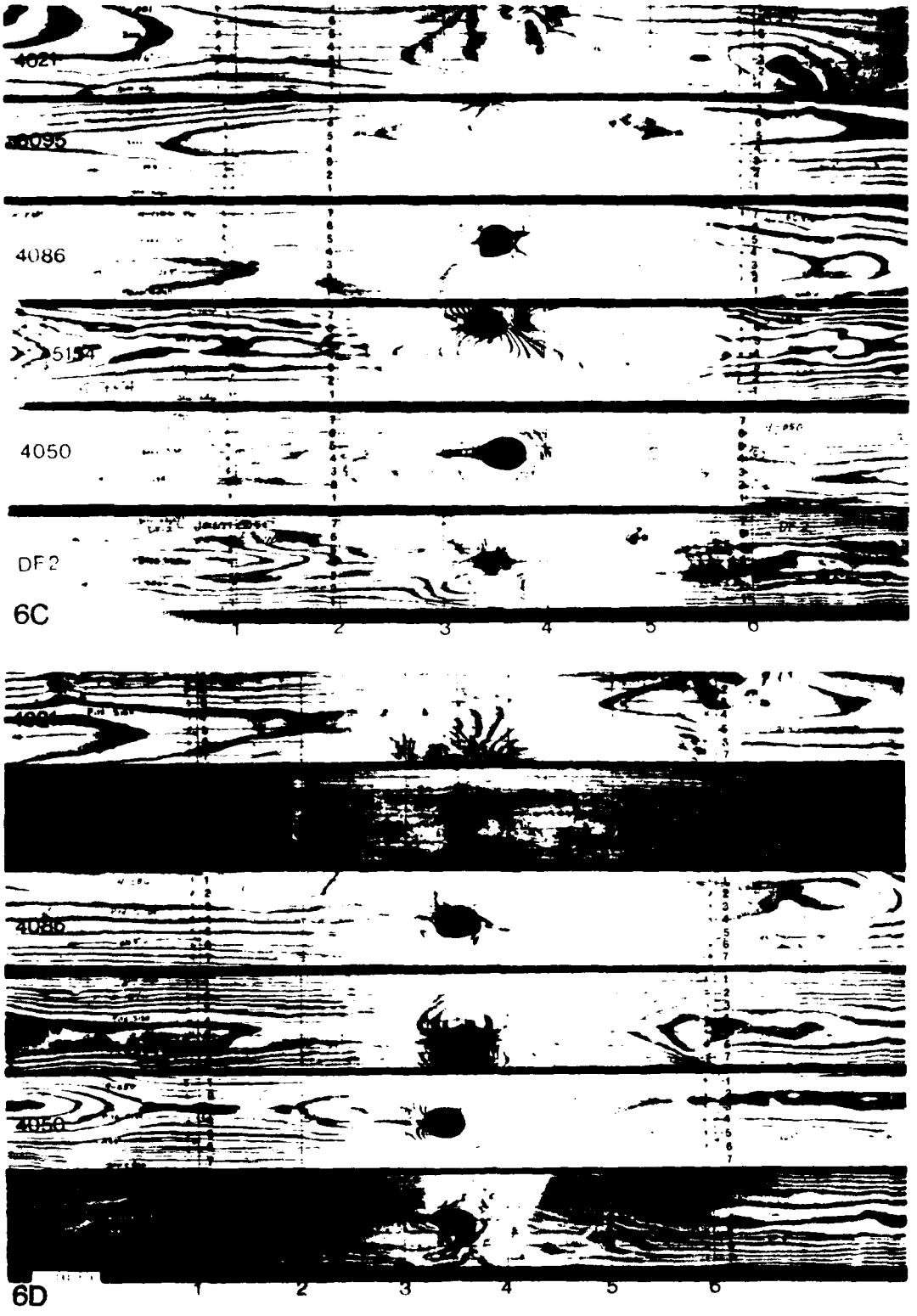

Figure 6 (continued).—Barkside and pithside views of the eleven 8 foot long 2 × 6's. Inscribed on each specimen are seven 3/4-inch grid lines (type set numbers) and six 6-inch cross-section lines over the 2-1/2-foot test section. C. barkside and D. pithside of 4021, 6095, 4086, 5154, 4050, and DF2. M 141 251, M 141 252

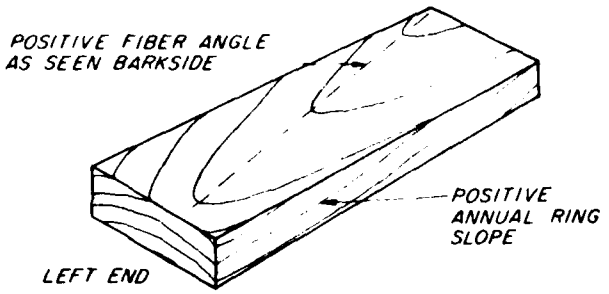

Figure 7.— Schematic showing positive slopes of fiber angle and annual rings. M 148 972

36 inches from the left end. The knot was intergrown on the pithside and partly intergrown on the barkside. Annual ring slope was very shallow but the fiber angle had a variable positive slope, averaging about 1 in 9 but ranging between 1 in 3-1/2 to 1 in 16 and tending to be steeper on the pithside than on the barkside. The specimen also had a short surface check on the barkside in the grain sloping around the right side of the knot.

Specimen 5154.—The prominent knot, 1.68 inches in diameter and encased, was partly overgrown on the barkside. It was located 28 inches from the left end on the edge of the piece. A very small corner knot was located about 14 inches to the right of the prominent knot. Fiber angle and annual ring slopes were essentially nil, except for the 1-foot length to the right of the knot and in a 2-foot length toward the right end on the barkside that had about 1 in 14 positive fiber angle slope.

Specimen 4050.—The prominent knot, 1.54 inches in diameter and completely intergrown, was located about 44-1/2 inches from the left end very slightly off midwidth. Fiber angle and annual ring slope were essentially nil.

Appendix B: Individual Specimen Contour Descriptions

Figures 8 through 12 contain several examples of stress wave contours estimated from equation (4) of the text. These examples show how the stress wave contours changed as width was reduced from 5-1/2 inches to 1-3/4 inches. While the examples represent results for stress wave transit from left to right (impact on left end), the opposite direction of transit is also shown for one specimen (5154).

Before individual specimen contours are discussed, an explanation of the appendix figures may be of help in understanding the stress-wave contours. The number given at a cross section (CX) between barkside and pithside contours is the average ($\bar{t}$) of transit times in microseconds to both barkside and pithside grid points equidistant from the hammer end for a given width of specimen. By comparing the $\bar{t}$'s in the appended figure for any one specimen, it is obvious that the $\bar{t}$'s for a given distance d differ slightly among the different specimen widths. Another point to note for clarity is that, for a given $\bar{t}$, the farthest advance of the stress wave is denoted by the point on the contour that is farthest away from the hammer end. The plus signs shown near the contours represent the "fastest points" of the stress wave contours located by trial and error. Stress-wave contours for individual specimens generally tend to show that stress waves are affected by knots, slope of grain, and slope of annual rings.

Specimen 4050—Contours for specimen 4050 (fig. 8) generally reflect an absence of cross grain except for grain associated with the knot. In travelling from the left end of 4050, the stress wave had a nearly normal contour about the first 6-inch CX (29.5 inches from the hammer end) and a slightly sloping contour about the second 6-inch CX line, regardless of specimen width. At the third 6-inch CX, just before the knot, the contour had a lagging tendency along 3/4-inch grid lines 4 and 5 on the barkside and 4 on the pithside. The lagging tendency, apparently associated with the annual ring tendency to slope around the knot, was more prominent behind the knot (about the fourth 6-inch CX line) thus demonstrating the accumulated influence of the knot and slope of grain both in front and behind the knot. As long as the knot was not completely ripped away, the knot influence was apparent, except on the pithside for 3-1/4 and 2-1/2-inch widths. By the fifth and sixth 6-inch CX line, the contours lack any strong evidence of knot influence. Note the contour about the fourth 6-inch grid line tended to lead on the pithside and lag on the barkside, apparently in association with the annual ring slope around the knot. The leading and lagging tendency was not apparent in the contours nearer the hammer end.

Specimen 5153—The contours of specimen 5153 (fig. 9) reflect the influence of both the knot and the annual ring slope near the knot. The contours about the first 6-inch CX line tended to be nearly normal on the barkside but somewhat sloped on the pithside reflecting a negative slope to the grain, with the trend holding regardless of specimen width. By the second 6-inch CX line, the stress-wave contour was nearly normal on both sides of the specimen regardless of specimen width. The contour about the third 6-inch grid line tended to lead on the barkside and lag on the pithside, apparently in association with the annual ring slope just before the knot. After passing the knot, the stress-wave contour generally led on the pithside and lagged on the barkside regardless of specimen width, mainly due to the direction and relatively steep slope of the annual rings immediately to the right of the knot.

The stress-wave contour about the fourth 6-inch CX line of 5153 also reflected the effect of the knot, strongly lagging along the 3/4-inch grid lines in line with the knot. That stress-wave contour calculated from equation (4) probably misrepresents the true contour shape, as the true contour probably would have curved around the knot rather than through the knot as shown. The contours about the fifth and sixth 6-inch CX lines appeared to reflect the knot and the slope of the fibers noted earlier for the right end of the specimen, as evidenced by the sloping contours even after the knot was ripped away (3-1/4-in. width and less).

Specimen DFI—The contours of DFI (fig. 10) tend to reflect the effect of a general positive fiber angle but the effects of the knot and the tree crook to the right of the knot are also evident. The cause of the early advance in the contour (23.2 to 35.2 inches from the hammer end) along midwidth on the barkside for the full-width specimen is not apparent, although it could have occurred if the specimen was cupped due to the interaction of cup and stress wave instrument used (2). The influence of the knot was evident as a retardation in the contour about the fourth 6-inch CX line in line with the knot, particularly when compared with the shape of the contour before the knot (about the third 6-inch CX line). That influence was apparent down through a specimen width of 2-1/2-inches. The tree-crook influence was evidenced by the general tendency for the stress-wave contour to lead on the barkside and lag on the pithside about the fifth 6-inch CX line; this response was in conjunction with the positive sloping characteristic of the annual rings starting to the right of the fourth 6-inch CX line and running through the fifth 6-inch CX line.

Specimen 5154—Stress-wave contours are shown for hammer end both to the left and to the right of the knot for specimen 5154. With the left end to the hammer (fig. 11), the stress-wave contour appeared to be nearly normal before it reached the knot (the first three 6-inch CX

lines). After passing the knot, however, the contours indicated that the stress wave was strongly affected by the knot so long as the knot was not ripped completely away. The contours about the fifth and sixth 6-inch CX lines must have continued to reflect the influence of the knot because the slope of the fibers to the right of the knot should have caused the contour to slope in the direction opposite to that shown. The stress-wave contours did not suggest any strong tendency toward leading or lagging on either side of the specimen, except for the leading pithside tendency at the fourth 6-inch CX line for the full width specimen.

With hammer end to the right, the contours for specimen 5154 (fig. 12) were quite different in appearance to those for hammer end to the left. With hammer end to the right, the stress wave advanced from the sixth to the first 6-inch CX line. In doing so, the stress wave was strongly affected by the slope of the fibers noted for the right end of the specimen as shown by the sloping contours about the sixth, fifth and fourth 6-inch CX lines, regardless of specimen width. The influence of the knot on the stress wave was reflected by the slope of the contours about the third 6-inch CX line, at least for the full and 4-3/4-inch specimen widths. After the knot had been ripped from the specimen, the stress-wave contours beyond 70 inches from the hammer end tended to become normal to the piece, reflecting the straighter grain to the left of the knot. Somewhat in contrast to the contours for the left end to the hammer, the stress-wave contours with the right end to the hammer strongly led on the barkside about the fourth 6-inch CX line and on the pithside about the third 6-inch CX line, regardless of specimen width.

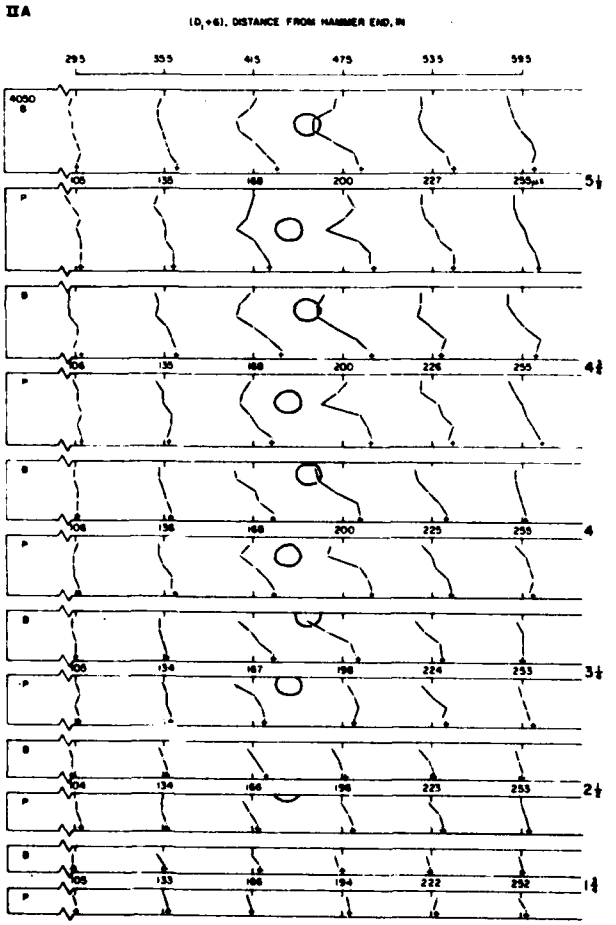

Figure 8.—Specimen 4050. Estimated stress-wave contours of constant time as specimen width is reduced by ripping. "B" denotes barkside and "P" pithside. Numbers in μs represent t̄. Knots are shown relative to specimen length and width.
M 148 973

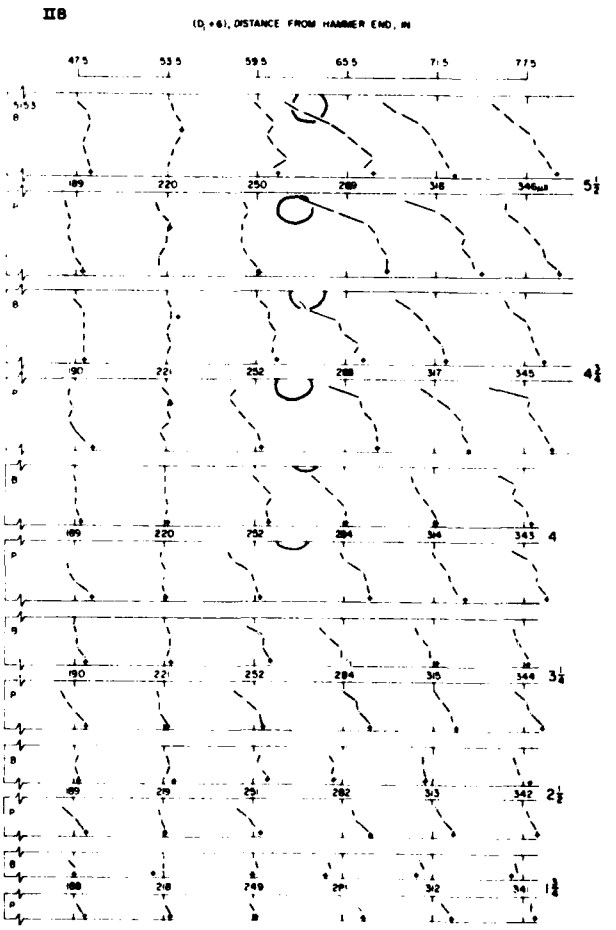

Figure 9.—Specimen 5153. Estimated stress-wave contours of constant time as specimen width is reduced by ripping. "B" denotes barkside and "P" pithside. Numbers in μs represent t̄. Knots are shown relative to specimen length and width.
M 148 974

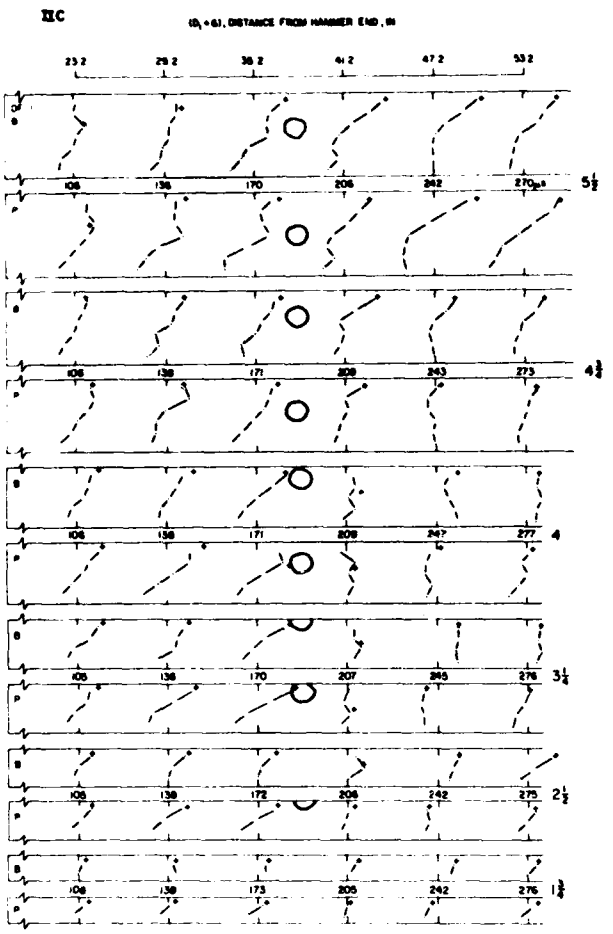

Figure 10.—Specimen DF 1. Estimated stress-wave contours of constant time as specimen width is reduced by ripping. "B" denotes barkside and "P" pithside. Numbers in μs represent $\bar{t}$. Knots are shown relative to specimen length and width.
M 148 975

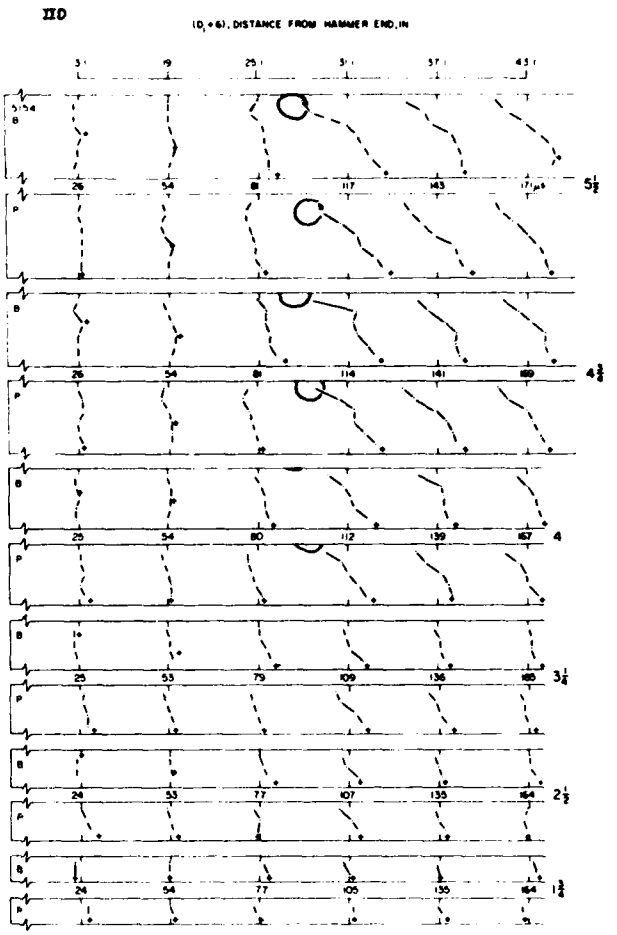

Figure 11.— Specimen 5154. Impact on left end. Estimated stress-wave contours of constant time as specimen width is reduced by ripping. "B" denotes barkside and "P" pithside. Numbers in μs represent $\bar{t}$. Knots are shown relative to specimen length and width.
M 148 976

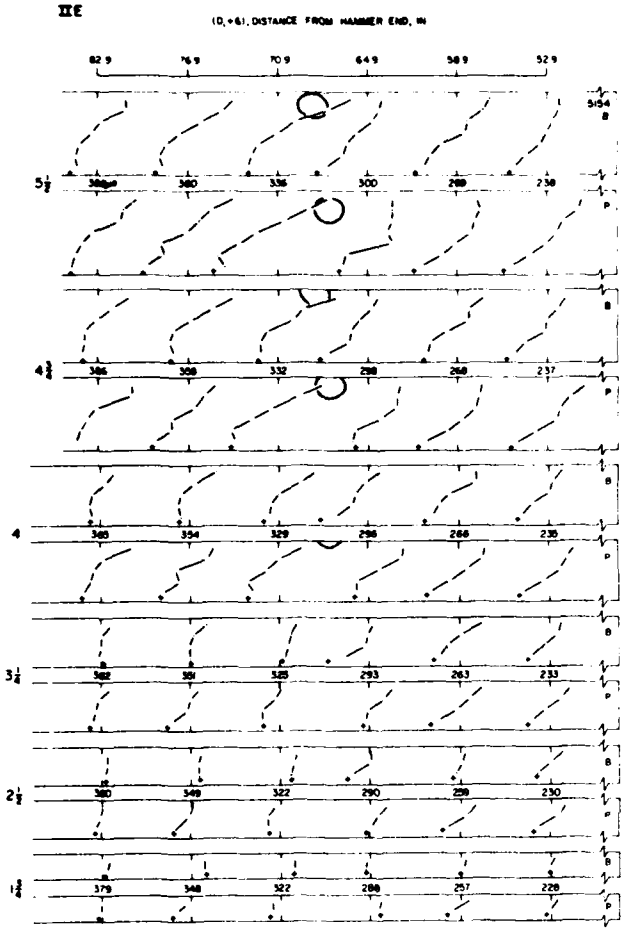

Figure 12.— Specimen 5154. Impact on right end. Estimated stress-wave contours of constant time as specimen width is reduced by ripping. "B" denotes barkside and "P" pithside. Numbers in μs represent t. Knots are shown relative to specimen length and width.
M 148 977

Appendix C: Six-Inch Transit Times Based on Fastest Point, Average, and Centerline Timing.

Table 11.—Six-inch transit times based on fastest point timing to each 6-inch cross section

Specimen number	Approximate width	Transit times between 6-inch cross-section lines									
		Hammer end left					Hammer end right				
		2-1	3-2	4-3	5-4	6-5	1-2	2-3	3-4	4-5	5-6
	in.	μs					μs				
6047	5.50	27	26	33	30	27	25	28	26	30	27
	4.75	29	28	28	30	29	29	26	27	27	31
	4.00	28	27	29	28	29	28	27	27	28	29
	3.25	26	27	31	27	28	28	29	26	29	28
	2.50	28	27	29	29	24	28	27	27	25	32
	1.75	28	26	27	30	27	27	26	27	29	27
DF1	5.50	29	30	33	33	32	29	34	39	37	30
	4.75	31	31	35	38	30	28	37	38	37	28
	4.00	28	34	43	36	33	32	34	38	37	32
	3.25	30	31	44	35	33	30	35	37	38	30
	2.50	30	34	35	35	30	29	32	41	36	32
	1.75	33	34	32	34	37	27	33	38	37	32
4107	5.50	31	30	34	27	30	28	29	27	29	27
	4.75	27	30	31	29	30	28	30	27	31	26
	4.00	30	26	32	28	30	30	27	29	29	30
	3.25	28	28	31	25	33	26	32	26	30	28
	2.50	28	27	29	29	29	29	28	28	29	27
	1.75	29	28	31	28	28	29	29	27	30	28
5153	5.50	30	25	37	27	32	31	25	35	31	33
	4.75	32	29	32	29	30	30	25	38	28	33
	4.00	34	29	29	28	31	29	34	39	27	32
	3.25	32	29	29	31	30	28	26	35	27	33
	2.50	31	30	28	32	31	27	27	32	29	34
	1.75	32	32	27	31	31	31	24	33	30	33
6172	5.50	26	31	28	29	29	30	28	29	30	28
	4.75	24	34	28	28	27	29	28	32	26	28
	4.00	26	32	26	30	28	30	30	27	30	29
	3.25	25	31	26	30	29	31	28	25	31	31
	2.50	25	31	27	28	31	30	27	26	31	32
	1.75	26	32	26	29	32	30	29	30	29	26
DF2	5.50	27	26	25	27	25	28	27	29	27	29
	4.75	26	26	31	23	26	28	28	29	28	26
	4.00	26	26	29	26	24	26	31	27	29	24
	3.25	26	29	32	23	25	28	30	25	29	27
	2.50	25	26	32	27	26	30	27	27	27	28
	1.75	26	25	32	28	29	27	28	28	28	25
4021	5.50	22	37	32	31	33	30	29	30	31	34
	4.75	28	31	31	31	29	33	28	27	35	32
	4.00	29	31	30	33	28	32	28	30	31	33
	3.25	28	32	30	30	32	30	28	29	31	31
	2.50	30	33	31	31	31	32	31	27	31	34
	1.75	32	31	30	31	31	33	28	28	32	32
6095	5.50	26	27	29	29	28	27	27	30	28	30
	4.75	27	28	30	27	27	27	29	29	29	30
	4.00	28	26	31	28	27	27	27	33	29	28
	3.25	28	26	30	26	30	30	26	30	30	28
	2.50	26	28	30	27	29	29	29	31	27	31
	1.75	28	29	32	27	28	28	28	29	28	30

(Page 1)

Table 11.—Six-inch transit times based on fastest point timing to each 6-inch cross section—continued

Specimen number	Approximate width	Transit times between 6-inch cross-section lines									
		Hammer end left					Hammer end right				
		2-1	3-2	4-3	5-4	6-5	1-2	2-3	3-4	4-5	5-6
	In.	μs					μs				
4086	5.50	32	32	27	30	28	28	31	35	29	31
	4.75	30	33	32	26	30	30	29	36	30	29
	4.00	30	32	33	29	28	30	30	33	31	30
	3.25	31	31	31	28	29	28	32	33	29	31
	2.50	32	28	31	29	30	28	32	34	30	31
	1.75	29	31	29	30	34	29	32	34	29	31
5154	5.50	28	24	29	28	29	30	29	32	29	34
	4.75	27	23	32	28	28	31	28	34	28	32
	4.00	29	24	28	30	28	30	26	37	26	34
	3.25	29	24	29	28	29	28	26	39	25	34
	2.50	30	22	31	29	28	28	30	35	25	34
	1.75	30	22	29	29	28	26	33	32	25	35
4050	5.50	28	30	30	29	30	27	28	29	34	29
	4.75	28	29	31	29	28	25	31	29	33	27
	4.00	28	30	29	28	32	26	27	30	33	29
	3.25	28	30	32	26	30	26	28	30	33	29
	2.50	30	29	31	27	31	25	29	29	33	29
	1.75	28	30	30	29	30	26	28	29	34	29

(Page 2)

Table 12.—Six-inch transit times based on average timing to each 6-inch cross section

Specimen number	Approximate width	Transit times between 6-inch cross-section lines									
		Hammer end left					Hammer end right				
		2-1	3-2	4-3	5-4	6-5	1-2	2-3	3-4	4-5	5-6
	In.	μs					μs				
6047	5.50	28	28	30	29	27	27	27	30	29	28
	4.75	28	29	31	28	28	27	28	30	29	27
	4.00	27	29	31	28	27	26	27	30	29	29
	3.25	27	28	29	28	28	27	27	28	30	28
	2.50	26	29	28	30	27	27	27	27	28	28
	1.75	27	28	27	29	27	27	28	28	26	28
DF1	5.50	31	33	36	36	28	31	34	35	34	31
	4.75	32	33	37	35	30	31	36	35	36	31
	4.00	32	33	38	38	30	32	35	38	33	32
	3.25	32	34	36	38	31	29	36	35	34	32
	2.50	33	34	34	36	33	32	34	37	32	32
	1.75	32	35	32	37	34	32	35	37	32	30
4107	5.50	29	29	33	28	29	28	27	32	29	28
	4.75	28	28	35	27	28	27	27	34	29	28
	4.00	28	28	33	26	29	27	28	30	29	29
	3.25	29	28	30	28	29	28	29	29	28	29
	2.50	28	28	29	29	30	27	27	31	28	29
	1.75	30	28	30	29	28	28	29	28	29	29
5153	5.50	31	30	39	29	28	30	27	37	31	29
	4.75	31	31	36	29	28	31	27	35	31	28
	4.00	31	32	33	29	29	31	29	31	30	29
	3.25	31	31	32	31	29	31	29	31	30	28
	2.50	30	32	31	31	29	32	31	29	30	30
	1.75	31	30	32	31	29	31	32	29	30	29

(Page 1)

Table 12.—Six-inch transit times based on average timing to each 6-inch cross section—continued

Specimen number	Approximate width	Transit times between 6-inch cross-section lines									
		Hammer end left					Hammer end right				
		2-1	3-2	4-3	5-4	6-5	1-2	2-3	3-4	4-5	5-6
	In.	μs					μs				
6172	5.50	29	30	30	28	29	30	27	31	28	31
	4.75	27	32	30	27	28	30	26	31	29	30
	4.00	29	30	29	28	28	31	28	29	29	30
	3.25	29	28	29	29	28	30	29	28	28	31
	2.50	28	29	28	30	28	30	31	26	28	31
	1.75	27	31	27	29	30	28	29	29	29	30
DF2	5.50	26	27	29	27	26	26	28	28	28	26
	4.75	27	27	30	27	26	26	27	29	28	27
	4.00	26	28	30	27	26	24	28	28	30	26
	3.25	27	27	31	27	26	26	29	27	28	27
	2.50	27	25	31	28	29	26	28	28	27	28
	1.75	28	25	31	27	30	25	28	27	28	28
4021	5.50	28	34	32	32	30	31	30	32	31	30
	4.75	29	31	31	31	30	29	31	31	30	31
	4.00	29	31	31	31	31	30	31	31	29	31
	3.25	28	30	31	31	31	30	31	30	29	31
	2.50	30	32	31	31	33	32	31	29	31	30
	1.75	32	32	31	31	33	31	32	29	29	32
6095	5.50	26	28	31	29	29	28	28	32	30	27
	4.75	26	28	32	28	28	29	28	31	30	28
	4.00	28	26	31	28	28	29	28	32	29	27
	3.25	28	26	31	27	28	28	29	32	28	29
	2.50	27	28	31	27	26	27	29	32	29	27
	1.75	28	28	30	27	29	28	29	29	29	28
4086	5.50	30	31	33	30	29	31	30	36	32	29
	4.75	30	31	35	27	31	32	30	35	32	29
	4.00	30	31	39	26	30	31	29	37	33	29
	3.25	30	30	34	30	29	31	29	32	34	30
	2.50	31	28	33	31	29	30	30	31	34	30
	1.75	31	29	31	33	29	30	31	30	35	29
5154	5.50	28	27	36	26	28	28	24	36	31	30
	4.75	28	27	33	27	28	28	26	34	30	31
	4.00	29	26	32	27	28	31	25	33	30	31
	3.25	28	26	30	28	28	31	26	32	30	30
	2.50	29	24	30	28	29	31	27	32	31	29
	1.75	29	23	28	30	29	30	27	34	31	29
4050	5.50	30	33	32	27	28	29	31	33	30	27
	4.75	29	33	32	26	29	29	30	34	30	27
	4.00	29	33	32	25	30	29	31	32	30	28
	3.25	29	33	31	26	29	29	30	34	29	27
	2.50	29	32	30	27	30	30	31	32	29	26
	1.75	28	31	30	29	29	29	33	31	27	27

(Page 2)

Table 13.—Six-inch transit times based on centerline timing to either the barkside or the pithside to each 6-inch cross-section line

Specimen number	Side of specimen	Approximate width	Transit times between 6-inch cross-section lines									
			Hammer end left					Hammer end right				
			2-1	3-2	4-3	5-4	6-5	1-2	2-3	3-4	4-5	5-6
		In.	μs					μs				
6047	Bark	5.50	28	28	32	28	26	25	26	33	33	28
		4.00	26	29	28	32	26	27	27	29	31	28
		2.50	27	28	29	28	27	25	29	27	29	27
	Pith	5.50	28	27	33	27	28	26	27	28	30	28
		4.00	28	28	27	30	28	26	26	28	29	29
		2.50	26	29	28	30	28	29	26	25	27	27
DF1	Bark	5.50	30	30	43	33	30	31	30	35	36	36
		4.00	33	34	37	35	29	33	32	38	31	36
		2.50	31	34	30	37	36	34	33	36	33	35
	Pith	5.50	29	34	46	40	21	30	31	33	39	29
		4.00	32	33	39	43	26	35	36	35	34	32
		2.50	35	33	34	39	30	33	33	37	33	27
4107	Bark	5.50	32	26	36	27	28	29	25	37	26	29
		4.00	29	27	33	26	30	31	27	31	28	30
		2.50	28	28	28	28	30	28	26	32	28	29
	Pith	5.50	29	31	29	28	33	25	32	28	30	29
		4.00	29	29	31	25	30	25	30	27	30	29
		2.50	29	28	28	31	28	27	28	29	27	30
5153	Bark	5.50	29	32	42	30	25	30	24	45	26	26
		4.00	31	27	40	31	28	32	29	35	25	27
		2.50	29	32	35	31	28	37	28	33	25	27
	Pith	5.50	28	35	26	29	35	34	26	26	40	31
		4.00	29	33	26	31	29	30	30	27	35	29
		2.50	31	32	27	31	30	27	32	27	33	29
6172	Bark	5.50	29	35	28	26	27	27	25	36	29	31
		4.00	27	32	27	28	28	30	27	30	29	31
		2.50	27	32	25	31	26	29	31	28	28	32
	Pith	5.50	29	30	32	25	27	36	26	28	26	30
		4.00	30	29	29	28	27	32	30	24	30	27
		2.50	32	25	31	30	28	30	31	24	29	30
DF2	Bark	5.50	24	33	27	24	27	26	28	23	32	28
		4.00	25	29	30	27	24	24	28	27	28	27
		2.50	26	24	32	28	28	25	29	27	28	25
	Pith	5.50	25	30	33	25	20	27	25	36	27	25
		4.00	27	26	32	28	28	27	27	29	32	26
		2.50	29	26	28	29	29	26	27	29	28	29
4021	Bark	5.50	29	32	33	32	29	30	30	35	32	30
		4.00	31	29	32	32	31	29	29	38	28	32
		2.50	31	30	30	32	33	32	31	32	28	33
	Pith	5.50	24	35	31	33	29	34	30	26	34	29
		4.00	28	32	29	32	32	30	32	26	33	28
		2.50	29	31	33	32	32	33	30	27	33	25
6095	Bark	5.50	27	26	32	31	28	31	27	31	32	26
		4.00	27	27	34	26	27	28	28	34	30	26
		2.50	25	29	32	27	28	30	28	32	28	28
	Pith	5.50	27	28	32	25	32	28	32	30	28	27
		4.00	28	27	33	26	27	29	28	32	29	29
		2.50	28	27	30	28	24	23	32	32	26	26
4066	Bark	5.50	31	26	41	25	30	30	25	46	28	26
		4.00	27	30	39	25	32	36	27	37	33	30
		2.50	29	31	33	30	30	30	31	33	32	30
	Pith	5.50	29	33	29	29	33	33	24	36	35	29
		4.00	31	31	33	31	32	38	28	30	36	29
		2.50	31	28	30	31	32	32	30	24	40	26

(Page 1)

Table 13.—Six-inch transit times based on centerline timing to either the barkside or the pithside to each 6-inch cross-section line—continued

Specimen number	Side of specimen	Approximate width	Transit times between 6-inch cross-section lines									
			Hammer end left					Hammer end right				
			2-1	3-2	4-3	5-4	6-5	1-2	2-3	3-4	4-5	5-6
		In.	μs					μs				
5154	Bark	5.50	28	26	35	25	29	29	21	40	25	33
		4.00	28	25	33	26	28	31	23	37	29	28
		2.50	28	23	32	27	29	30	25	36	31	29
	Pith	5.50	30	28	31	30	27	27	30	23	33	32
		4.00	30	38	30	26	30	33	25	26	31	30
		2.50	30	24	29	29	31	31	30	26	32	28
4050	Bark	5.50	30	36	37	21	26	27	28	37	34	28
		4.00	31	32	34	24	30	26	33	34	31	27
		2.50	29	31	32	27	30	30	30	32	29	27
	Pith	5.50	30	38	32	21	29	28	26	38	29	28
		4.00	30	32	27	29	29	32	34	27	32	27
		2.50	30	32	28	27	31	30	33	30	29	25

(Page 2)

Appendix D

Appendix D.—Modulus of elasticity values for 2-foot portions of the 2-1/2-foot test section

Specimen number	Approximate width	ESB		ESW (Left end to hammer)							
				Fastest point		Average		Centerline			
		Left 2-foot span	Right 2-foot span	Left 2-foot span	Right 2-foot span	Left 2-foot span	Right 2-foot span	Barkside		Pithside	
								Left 2-foot span	Right 2-foot span	Left 2-foot span	Right 2-foot span
	In.	10^6 lb/in.^{2}									
6047	5.50	1.98	1.97	2.23	2.23	2.26	2.28	2.23	2.31	2.27	2.27
	4.75	1.88	1.91	2.28	2.28	2.22	2.24				
	4.00	1.82	1.86	2.39	2.34	2.26	2.28	2.26	2.26	2.34	2.34
	3.25	2.04	2.04	2.45	2.36	2.37	2.37				
	2.50	2.26	2.23	2.38	2.56	2.39	2.38	2.43	2.38	2.43	2.30
	1.75	2.36	2.31	2.48	2.52	2.47	2.48				
DF1	5.50	1.68	1.58	2.19	2.09	1.84	1.92	1.85	1.85	1.54	1.72
	4.75	1.61	1.51	1.88	1.91	1.84	1.87				
	4.00	1.48	1.41	1.71	1.59	1.71	1.75	1.75	1.86	1.57	1.71
	3.25	1.60	1.51	1.75	1.67	1.74	1.76				
	2.50	1.67	1.58	1.91	1.91	1.82	1.82	1.97	1.82	1.72	1.85
	1.75	1.66	1.66	1.96	1.84	1.87	1.82				
4107	5.50	1.79	1.75	1.95	1.99	2.06	2.04	1.99	2.12	2.12	1.99
	4.75	1.73	1.72	2.13	2.02	2.09	2.07				
	4.00	1.80	1.80	2.15	2.15	2.19	2.15	2.19	2.15	2.23	2.19
	3.25	1.89	1.92	2.30	2.10	2.20	2.18				
	2.50	1.96	1.98	2.24	2.20	2.19	2.13	2.28	2.20	2.13	2.17
	1.75	1.97	2.03	2.14	2.18	2.12	2.17				
5153	5.50	1.16	1.20	1.90	1.84	1.62	1.67	1.52	1.62	1.93	1.72
	4.75	1.18	1.23	1.81	1.88	1.65	1.75				
	4.00	1.26	1.31	1.87	1.97	1.73	1.79	1.62	1.70	1.90	1.90
	3.25	1.34	1.39	1.82	1.88	1.70	1.76				
	2.50	1.39	1.46	1.84	1.84	1.76	1.80	1.67	1.70	1.84	1.88
	1.75	1.45	1.54	1.83	1.86	1.77	1.81				
6172	5.50	1.56	1.54	2.16	2.05	2.07	2.03	2.01	2.08	2.08	2.16
	4.75	1.53	1.51	2.16	2.05	2.08	2.05				
	4.00	1.55	1.56	2.17	2.10	2.11	2.13	2.17	2.13	2.10	2.21
	3.25	1.63	1.67	2.26	2.11	2.12	2.18				
	2.50	1.78	1.81	2.35	2.11	2.19	2.21	2.19	2.22	2.08	2.22
	1.75	1.94	1.95	2.31	2.08	2.26	2.17				
DF2	5.50	2.33	2.38	2.82	2.93	2.62	2.61	2.66	2.52	2.43	2.66
	4.75	2.26	2.32	2.78	2.78	2.54	2.56				
	4.00	2.13	2.21	2.67	2.77	2.47	2.50	2.48	2.52	2.39	2.35
	3.25	2.06	2.05	2.52	2.57	2.42	2.46				
	2.50	2.25	2.27	2.60	2.55	2.54	2.49	2.60	2.50	2.50	2.50
	1.75	2.34	2.31	2.44	2.32	2.46	2.33				
4021	5.50	1.55	1.56	1.88	1.58	1.78	1.72	1.77	1.77	1.85	1.71
	4.75	1.58	1.60	1.92	1.89	1.88	1.84				
	4.00	1.64	1.60	1.88	1.91	1.90	1.85	1.85	1.85	1.94	1.82
	3.25	1.67	1.70	1.97	1.85	1.96	1.86				
	2.50	1.61	1.67	1.82	1.79	1.87	1.78	1.88	1.82	1.82	1.74
	1.75	1.62	1.66	1.87	1.90	1.84	1.79				

(Page 1)

Appendix D.—Modulus of elasticity values for 2-foot portions of the 2-1/2-foot test section

Specimen number	Approximate width	ESB		ESW (Left end to hammer)							
				Fastest point		Average		Centerline			
		Left 2-foot span	Right 2-foot span	Left 2-foot span	Right 2-foot span	Left 2-foot span	Right 2-foot span	Barkside		Pithside	
								Left 2-foot span	Right 2-foot span	Left 2-foot span	Right 2-foot span
	in.	10^6 lb/in.^{2}									
6095	5.50	2.06	1.94	2.77	2.68	2.63	2.51	2.54	2.50	2.72	2.50
	4.75	2.18	2.05	2.73	2.73	2.64	2.56				
	4.00	2.22	2.14	2.79	2.84	2.71	2.69	2.65	2.65	2.65	2.70
	3.25	2.23	2.17	2.89	2.79	2.79	2.81				
	2.50	2.30	2.25	2.90	2.75	2.80	2.85	2.80	2.65	2.80	3.01
	1.75	2.46	2.45	2.66	2.66	2.82	2.78				
4086	5.50	1.42	1.43	1.96	2.10	1.87	1.89	1.84	1.87	1.99	1.87
	4.75	1.38	1.35	1.96	1.96	1.89	1.86				
	4.00	1.33	1.30	1.86	1.92	1.80	1.81	1.95	1.80	1.80	1.77
	3.25	1.43	1.35	1.96	2.02	1.86	1.91				
	2.50	1.57	1.45	2.02	2.09	1.94	1.98	1.92	1.89	2.02	1.99
	1.75	1.75	1.59	2.01	1.85	1.87	1.93				
5154	5.50	1.72	1.63	2.86	2.81	2.47	2.47	2.62	2.57	2.40	2.53
	4.75	1.78	1.68	2.80	2.75	2.55	2.53				
	4.00	1.93	1.81	2.74	2.79	2.60	2.61	2.69	2.69	2.60	2.60
	3.25	2.05	1.93	2.76	2.76	2.67	2.67				
	2.50	2.20	2.11	2.67	2.77	2.73	2.69	2.77	2.72	2.67	2.62
	1.75	2.27	2.22	2.76	2.86	2.72	2.74				
4050	5.50	1.44	1.52	2.04	1.97	1.89	1.93	1.81	1.94	1.90	1.94
	4.75	1.36	1.44	2.03	2.03	1.90	1.93				
	4.00	1.32	1.41	2.11	1.97	1.96	1.96	1.90	1.94	2.00	2.04
	3.25	1.38	1.46	2.12	2.04	2.02	2.00				
	2.50	1.58	1.68	2.14	2.11	2.08	2.06	2.07	2.04	2.14	2.11
	1.75	1.68	1.74	2.03	1.96	2.01	1.96				

(Page 2)

Effect of knots on stress waves in lumber, by C. C. Gerhards. Madison, Wis., FPL, 1982.

28 p., (USDA For. Serv. Res. Pap. FPL 384).

An impact stress wave was induced in the end of 2 by 6 lumber containing knots. Stress wave modulus of elasticity (ESW) calculated from the data tended to be lowest with the average timing method. All ESW's were higher than static bending modulus of elasticity; however, the two types of moduli tended to approach each other as knots were removed. The results of this study should provide guidance in establishing stress wave methods for machine grading of lumber.